THE JOURNAL OF BIOLOGICAL CHEMISTRY VOL. 291, NO. 8, pp. 4019–4034, February 19, 2016
© 2016 by The American Society for Biochemistry and Molecular Biology, Inc. Published in the U.S.A.

Identification of the Zinc Finger Protein ZRANB2 as a Novel Maternal Lipopolysaccharide-binding Protein That Protects Embryos of Zebrafish against Gram-negative Bacterial Infections*[S]

Received for publication, July 15, 2015, and in revised form, December 31, 2015 Published, JBC Papers in Press, January 6, 2016, DOI 10.1074/jbc.M115.679167

Xia Wang[‡], Xiaoyuan Du[‡], Hongyan Li[‡1], and Shicui Zhang[‡§2]

From the [‡]Institute of Evolution and Marine Biodiversity and the Department of Marine Biology, Ocean University of China, Qingdao 266003, China and the [§]Laboratory for Marine Biology and Biotechnology, Qingdao National Laboratory for Marine Science and Technology, Qingdao 266003, China

Zinc finger ZRANB2 proteins are widespread in animals, but their functions and mechanisms remain poorly defined. Here we clearly demonstrate that ZRANB2 is a newly identified LPS-binding protein present abundantly in the eggs/embryos of zebrafish. We also show that recombinant ZRANB2 (rZRANB2) acts as a pattern recognition receptor capable of identifying the bacterial signature molecule LPS as well as binding the Gram-negative bacteria *Escherichia coli*, *Vibrio anguilarum*, and *Aeromonas hydrophila* and functions as an antibacterial effector molecule capable of directly killing the bacteria. Furthermore, we reveal that N-terminal residues 11–37 consisting of the first ZnF_RBZ domain are indispensable for ZRANB2 antimicrobial activity. Importantly, microinjection of rZRANB2 into early embryos significantly enhanced the resistance of the embryos against pathogenic *A. hydrophila* challenge, and this enhanced bacterial resistance was markedly reduced by co-injection of anti-ZRANB2 antibody. Moreover, precipitation of ZRANB2 in the embryo extracts by preincubation with anti-ZRANB2 antibody caused a marked decrease in the antibacterial activity of the extracts against the bacteria tested. In addition, the N-terminal peptide $Z_{1/37}$ or $Z_{11/37}$ with *in vitro* antibacterial activity also promoted the resistance of embryos against *A. hydrophila*, but the peptide $Z_{38/198}$ without *in vitro* antibacterial activity did not. Collectively, these results indicate that ZRANB2 is a maternal LPS-binding protein that can protect the early embryos of zebrafish against pathogenic attacks, a novel role ever assigned to ZRANB2 proteins. This work also provides new insights into the immunological function of the zinc finger proteins that are widely distributed in various animals.

Embryos of most mammalian species including our human being develop in the uterus inside the mother's body and are thus well protected from pathogenic attacks. By contrast, the eggs of most fish are released and fertilized externally, and the resulting embryos/larvae are exposed to a hostile aquatic environment full of potential pathogens capable of causing various types of diseases (1). For example, the bacterium *Flavobacterium psychrophilum* has been shown to be the cause of a bacterial cold water disease that can affect salmonids ranging from yolk sac to yearling fish (2), and the virus *Herpesvirus ictaluri* is the cause of channel catfish virus disease, an acute viremia, which may result in high mortality and stunting of fry in juvenile channel catfish (3). Recently, it has been shown that exposure of salmon fry and juveniles to the Gram-negative bacterium *Yersinia ruckeri* causes the occurrence of enteric redmouth disease, leading to 60% mortality (4). However, early developing fish embryos/larvae have little or only limited ability to synthesize immune relevant molecules endogenously, and their lymphoid organs are not fully formed (5, 6). Furthermore, the early embryonic developmental stage is one of the most vulnerable periods in the fish life history (7), making the embryos more susceptible to invading pathogens. How fish embryos/larvae survive the pathogenic attacks in such a hostile environment is an intriguing and thus far unsolved question.

Fish eggs are in most cases cleidoic, *i.e.* in a closed free-living system post-fertilization; they are therefore supposed to depend upon the maternal provision of immune relevant molecules for protection against potential pathogens before full maturation of adaptive immune system (8). In the past 2 decades, the massive increase in aquaculture has put a greater emphasis on studies of the immune system and defense mechanisms against diseases associated with fish. As a result, a great progress has been made in recent years on the defense roles of maternally derived factors in embryos and larvae in fishes. It has been shown that maternal IgM is able to be transferred from mother to offspring in several fish species (9–20). Likewise, maternal transfer of the innate immune factors including lectins (21–25), lysozymes (26–28), and the vitellogenin-derived yolk proteins phosvitin and lipovitellin (29, 30) to offspring has

* This work was supported by Grants 31372505 and U1401211 from the National Natural Science Foundation of China, by Grant 201562029 from the Fundamental Research Funds for Central Universities, and by the Laboratory for Marine Biology and Biotechnology, Qingdao National Laboratory for Marine Science and Technology, China. All experimental animals were treated in accordance with the guidelines of the Laboratory Animal Administration Law of China (permit number SD2007695) as approved by the Ethics Committee of the Laboratory Animal Administration of Shandong province. The authors declare that they have no conflicts of interest with the contents of this article.

[S] This article contains supplemental Figs. S1–S4 and Table S1.

[1] To whom correspondence may be addressed: Institute of Evolution and Marine Biodiversity and Dept. of Marine Biology, Ocean University of China, Qingdao 266003, China. Tel.: 86-532-82032092; E-mail: hongyanli@ouc.edu.cn.

[2] To whom correspondence may be addressed: Institute of Evolution and Marine Biodiversity and Dept. of Marine Biology, Ocean University of China, Qingdao 266003, China. Tel.: 86-532-82032787; E-mail: sczhang@ouc.edu.cn.

also been reported in different teleost species. Moreover, many of the complement components in fish, including C3, Bf, CD59, and C1q, are transferred from mothers to eggs at either the protein level or the mRNA level (31–36). Despite the enormous progress already made, we still have no idea how many maternal immune relevant factors are present in fish eggs, and the search for novel maternal immune molecules in fish eggs remains in its infancy. In this study, we have demonstrated that ZRANB2 is a newly identified maternal immune factor that can protect the embryos/larvae of zebrafish against Gram-negative bacterial infections. ZRANB2, originally identified from rat renal juxtaglomerular cells by Karginova *et al.* (37), has been isolated from a variety of vertebrates, including humans, mouse, rat, chicken, amphibians, and fish, and shown to be highly conserved among these species. Prior studies show that ZRANB2 proteins are co-immunoprecipitated with mRNAs and colocalized with the splicing factors SMN, U1–70K, U2AF35, and SC35, implying that ZRANB2 is a novel component of spliceosomes (38, 39). Recently, ZRANB2 has been characterized as a novel Smad-binding protein that suppresses bone morphogenetic protein (BMP) signaling (40) and is suggested to be a molecule associated with tumor development in mammals (41). Our study is thus the first report to show that ZRANB2 plays an immunological role in animals. This provides a new angle for the study of the immune functions and mechanisms of zinc finger proteins that are widely present in various animals.

Materials and Methods

Fish and Embryos—Wild-type zebrafish *Danio rerio* were purchased from a local fish dealer and maintained in the containers with well aerated tap water at 27 ± 1 °C. The fishes were fed with live bloodworms and fish flakes (TetraMin) twice a day. Sexually mature *D. rerio* were placed in the late evening at a female to male ratio of 2:1, and the naturally fertilized eggs were collected early the next morning and cultured at 27 ± 1 °C until use.

Isolation of LPS-bound Proteins and Mass Spectrometric Analysis—Lipopolysaccharide-conjugated affinity resin was prepared by coupling LPS (Sigma) from *Escherichia coli* O55:B5 with CNBr-activated Sepharose CL-4B (GE Healthcare) according to the manufacturer's instructions. A total of 300 embryos collected at cell stages 64 to 128 were washed three times with sterilized distilled water, homogenized, and centrifuged at 5000 × *g* at 4 °C for 10 min. The supernatant was filtered through a 0.2-mm pyrogen-free filter to remove insoluble substances. After the addition of protease inhibitors, the supernatant was loaded onto the column, which had been pre-equilibrated with the initial buffer (10 mM Tris-HCl with 150 mM NaCl, pH 7.4) and incubated at 4 °C overnight. The column was washed with at least 10 column volumes of the initial buffer to remove the impurities. To recover proteins from the affinity matrix, the column was eluted with the elution buffer (4 M urea in 10 mM Tris-HCl, pH 7.4) as described by Chiou *et al.* (42). The effluent fractions containing the adsorbed proteins were pooled, desalted by gel filtration on a Sephadex G-25 column, and then concentrated with an Ultrafree-MC 5,000 nominal molecular weight filter unit (Millipore). The entire isolation procedure was performed at 4 °C. The LPS-bound proteins obtained were separated by SDS-PAGE and visualized by silver staining according to the methods of Minoda *et al.* (43) and Choi *et al.* (44). For mass spectrometric analysis, the protein bands visualized with silver staining were cut from gels and digested with trypsin (sequencing grade, Promega). MALDI/TOF MS analysis was performed on a Bruker Ultraflex MALDI/TOF MS mass spectrometer (Bremen, Germany) and searched against the nonredundant protein sequence database of the National Center for Biotechnology Information (NCBI) using the Mascot search engine (Matrix Science).

Western Blotting—MALDI/TOF MS analysis revealed that one of the proteins was ZRANB2, which is highly conserved among different species (see below). To examine the distribution of ZRANB2 in the different tissues and at the different developmental stages, the kidney, heart, liver, spleen, gut, muscle, gill, eye, ovary, testis, brain, skin, and tail were dissected out of zebrafish, and the newly fertilized eggs and embryos were collected at 12 and 24 h post-fertilization (hpf).[3] All the samples were homogenized in PBS, pH 7.5, using a Polytron and sonicator, and the homogenates were centrifuged at 5,000 × *g* at 4 °C for 10 min. The protein concentration of the supernatants was determined using a bicinchoninic acid protein assay kit (ComWin Biotech). The supernatants were loaded onto and run on a 12% SDS-PAGE. The proteins on the gel were electroblotted onto PVDF membrane (Amersham Biosciences) by a semi-dry technique, and the blotted membranes were blocked with 4% bovine serum albumin (BSA) in PBS, pH 7.4, at room temperature for 2 h followed by incubation with rabbit anti-human ZRANB2 antibody (ZNF265 antibody, N-terminal region, ARP37747_T100) diluted 1: 800 with PBS, pH 7.4, at 4 °C overnight. The antibody was prepared from the peptide RCGREKTTEAKMMKAGGTEIGKTLAEKSRGLFSANDWQ-CKTCSNVNWARR, which shares 98% conservation with the corresponding sequence of zebrafish ZRANB2 (Aviva Systems Biology). After a thorough washing in PBS, pH 7.4, containing 0.1% Tween 20, the membranes were incubated in horseradish peroxidase (HRP)-labeled goat anti-rabbit IgG (ComWin Biotech) diluted 1:2000, at room temperature for 3 h. The bands were visualized using DAB (3,3′*N*-diaminobenzidine tetrahydrochloride) (ComWin Biotech).

Immunohistochemistry—To examine the localization of ZRANB2 in cells, the embryos at desired stages were fixed in 4% paraformaldehyde in PBS overnight and frozen in prechilled acetone at −20 °C for 30 min. The embryos were washed four times with PBS containing 0.5% Triton X-100 (PBST), blocked in PBST with 5% sheep serum, 1% BSA, and 1% dimethylsulfoxide for about 2 h, and then incubated with human anti-rabbit ZRANB2 antibody diluted 1:500 at 4 °C overnight. After washing four times with PBST for at least 1 h, the embryos were incubated in PBST with 5% sheep serum, 1% BSA, 1% dimethyl sulfoxide, and goat anti-rabbit Alexa 488 antibody diluted 1:200 at 4 °C overnight. For control, the embryos were similarly washed and incubated with rabbit preimmune serum. To stain

[3] The abbreviations used are: hpf, hours post-fertilization; qRT-PCR, semi-quantitative real time-PCR; WISH, whole-mount *in situ* hybridization; r, recombinant (*e.g.* rZRANB2); PRR, pattern recognition receptor; PDB, Protein Data Bank.

the nuclei, the embryos were counterstained with 1 μg/ml 4′,6-diamidino-2-phenylindole (DAPI) in PBS for 10 min, washed in PBST for 10 min, and stored at 4 °C. The embryos/larvae were observed and photographed under a Leica confocal microscope.

In parallel, 24-hpf larvae were fixed in 4% polyformaldehyde in PBS and precipitated in a 30% sucrose solution at 4 °C overnight. Subsequently, they were embedded in optical cutting temperature compound, and sections were cut at 14 μm thickness at −20 °C (Leica). The sections were stained as described above, observed, and photographed under a Leica confocal microscope.

Cloning and Sequencing of Zebrafish zranb2—A total of 60 embryos/larvae of zebrafish was collected at about the 128-cell stage and ground in RNAiso Plus (TaKaRa). Total RNA were isolated from the ground samples according to the manufacturer's instructions (Omega). After digestion with recombinant DNase I (RNase-free) (TaKaRa) to eliminate genomic contamination, the cDNA were synthesized with a reverse transcription kit (TaKaRa) with an oligo(dT) primer. The reaction was carried out at 42 °C for 1 h and inactivated at 75 °C for 15 min. The cDNA were stored at −20 °C till used.

Based on the sequence of zebrafish *zranb2* (AAH52752.1) on NCBI, a primer pair, zranb2S and zranb2A, specific for *zranb2* (Table 1), was designed using the Primer Premier program, version 5.0, and used for PCR to amplify the ZRANB2 cDNA using the RNA isolated above. The PCR protocol was as follows: an initial denaturation at 94 °C for 5 min followed by 37 cycles of 94 °C for 30 s, 55 °C for 30 s, and 72 °C for 40 s and a final extension at 72 °C for 7 min. The amplification product was cloned into the pGEM-T vector (Tiangen Biotech) following the manufacturer's instructions and transformed into Trans 5α bacteria (TransGen Biotech). The DNA inserts were sequenced to verify for authenticity.

Homology, Phylogenetics, and Synteny Analyses—The ZRANB2 cDNA obtained was analyzed for coding probability with the DNASTAR software package, version 5.0, and the protein domain analyzed using the SMART program. The signal peptide prediction was conducted using the Signal P 3.0 server, and the molecular mass and isoelectronic point (pI) of the mature peptide were determined using ProtParam. The nuclear localization signal was predicted by PSORT II, and the three-dimensional structure prediction was performed by SWISS-MODEL online software at the Expert Protein Analysis System using residues 1–40 (PDB code: 1n0z.1.A) and residues 65–95 (PDB code: 2k1p.1.A) of human ZRANB2 as the model.

Homology searches in the GenBank™ database were carried out using the BLAST server, and multiple alignments of the protein sequences were generated using the ClustalW program (45) within MegAlign of the DNASTAR software package, version 5.0. The phylogenetic tree was constructed by MEGA, version 4.0, using p-distance based on the neighbor-joining method. The reliability of each node was estimated by bootstrapping with 1000 replications. Chromosomal locations of human (*Homo sapiens*), cow (*Bos taurus*), mouse (*Mus musculus*), frog (*Xenopus tropicalis*), and zebrafish (*D. rerio*) *zranb2* genes were obtained from the Sequence Viewer and Ensembl genome browser.

Assay for Expression Patterns of zranb2—To detect the expression patterns of *zranb2* in different tissues and at different developmental stages, the tissues including the kidney, heart, liver, spleen, gut, muscle, gill, eye, ovary, testis, brain, skin, and tail as well as the embryos/larvae, including the newly fertilized eggs, 4-, 16-, and 256-cell-stage embryos (~1, 1.5, and 2.5 hpf), high blastula-stage embryos (~3.5 hpf), 50% epiboly-stage embryos (~5 hpf), 10-somite-stage embryos (~15 hpf), 2-day-old larvae, and 3-day-old larvae, were sampled, ground in RNAiso Plus (TaKaRa), and stored at −70 °C until use. RNA extraction and cDNA synthesis were processed as described above. The semiquantitative real time-PCR (qRT-PCR) was performed in a final volume of 20 μl of the reaction mixture consisting of 10 μl of SYBR Premix Ex Taq™ (Tli RNase H Plus), 0.4 μl of ROX reference dye II, 0.5 μl of template, and each the sense and antisense primers (200 nM), qzranb2S and qzranb2A, specific for *zranb2*, designed using the Primer Premier program. The β-actin gene was chosen as the reference for internal standardization. All of the qRT-PCR experiments were conducted in triplicate and repeated three times. The amplification was performed on an ABI 7500 real-time PCR system (Applied Biosystems) initially at 95 °C for 15 s followed by 40 cycles of 95 °C for 5 s, 60 °C for 15 s, and 72 °C for 35 s. The expression levels of *zranb2* relative to that of the β-actin gene were calculated by the comparative Ct method (46).

Whole-mount in Situ Hybridization (WISH)—The embryos/larvae were collected at the 2-cell stage, 256-cell stage, 50% epiboly stage, 10-somite stage, 1, 2, 3, and 5 days post-fertilization. A fragment of *zranb2* was PCR-amplified using the primer pair wzranb2S and wzranb2A (Table 1) and subcloned into vector pGEM-T. The constructed vector was digested by the NcoI enzyme, and the *zranb2*-specific antisense probe labeled with digoxigenin-linked nucleotides was synthesized by Sp6 RNA polymerase. WISH was performed as described by C. Thisse and B. Thisse (47). Embryos/larvae were fixed and permeabilized before being soaked in the digoxigenin-labeled probe. After washing away the excess probe, the hybrids were detected by immunohistochemistry using an alkaline phosphatase-conjugated antibody against digoxigenin and a nitro blue tetrazolium/5-bromo-4-chloro-3-indolyl phosphate (NBT/BCIP) substrate. The embryos/larvae were observed and photographed under a stereomicroscope (Nikon).

Expression and Purification of rZRANB2—The cDNA encoding complete ZRANB2 was amplified by PCR using the sense primer rzranb2S (BamHI site is underlined) and the antisense primer rzranb2A (HindIII site is underlined) (Table 1). The reaction was carried out under the following conditions: initial denaturation at 94 °C for 5 min followed by 35 cycles of denaturation at 94 °C for 30 s, annealing at 55 °C for 30 s, extension at 72 °C for 40 s, and an additional extension at 72 °C for 7 min. The PCR products were digested with BamHI and HindIII and subcloned into the pET28a expression vector (Novagen, Darmstadt, Germany) digested previously with the same restriction enzymes. The inserts were verified by DNA sequencing, and the expression constructs were designated *pET28a/zranb2*.

The cells of *E. coli* BL21(DE3) were transformed with the plasmid *pET28a/zranb2* and then cultured in LB broth containing 100 μg/ml kanamycin, which is a protein biosynthesis

inhibitor combining with 30s ribosome and can cause mRNA password misreading (The plasmid *pET28a/zranb2* is resistant to kanamycin, and thus *E. coli* BL21 with the plasmid *pET28a/zranb2* can readily synthesize the protein). The cultures were incubated in ZYM-0.8G for about 6 h, diluted at 1:100 with ZYM-5052, and then subjected to further incubation overnight at 37 °C. The bacterial cells were harvested by centrifugation at 5,000 × *g* at 4 °C for 10 min, resuspended in ice-cold lysis buffer (50 mM Tris-HCl containing 100 mM NaCl, pH 7.5), and sonicated on ice. The homogenate was centrifuged at 12,000 × *g* at 4 °C for 30 min, and the supernatant was collected. The protein rZRANB2 was purified by nickel-nitrilotriacetic acid resin column (GE Healthcare). Purified rZRANB2 was analyzed by SDS-PAGE on a 12% gel and stained with Coomassie Brilliant Blue R-250. In parallel, the purified rZRANB2 was also characterized by Western blotting. Protein concentration was determined by the bicinchoninic acid method using BSA as a standard (ComWin Biotech).

Assay for Binding of rZRANB2 to LPS, Lipid A, and Bacteria—Both rZRANB2 and BSA were individually biotinylated with biotinamidohexanoic acid *N*-hydroxysuccinimide ester (NHS-LC-biotin; HEOWNS Biochem Technologies, Tianjin, China) as described by Zhang *et al.* (48). To verify the binding of rZRANB2 to LPS, 50 μl of 80 μg/ml LPS in 10 mM PBS, pH 7.4, was applied to each well of a 96-well microplate and air-dried at 25 °C overnight. The plate was incubated at 60 °C for 30 min to further fix the LPS, and the wells were each blocked with 200 μl of 1 mg/ml BSA in 10 mM PBS, pH 7.4, at 37 °C for 2 h. After washing four times with 200 μl of 10 mM PBS supplemented with 0.5% Tween 20, 50 μl of biotinylated rZRANB2 or BSA (0, 0.35, 0.7, 1.4, 3.5, 7, and 14 μg/ml) was added to each well. After incubation at room temperature for 3 h, the wells were each rinsed four times with 200 μl of 10 mM PBS supplemented with 0.5% Tween 20, and 100 μl of streptavidin-HRP (ComWin Biotech) diluted to 1:5000 with 10 mM PBS, pH 7.4, containing 1 mg/ml BSA was added to each well. After incubation at room temperature for 1 h, the wells were washed four times with 200 μl of 10 mM PBS supplemented with 0.5% Tween 20, added with 75 μl of 0.4 mg/ml *O*-phenylenediamine (Amresco) in a buffer consisting of 51.4 mM Na_2HPO_4, 24.3 mM citric acid, and 0.045% H_2O_2, pH 5.0, and reacted at 37 °C for 5 to 30 min. Subsequently, 25 μl of 2 M H_2SO_4 was added to each well to terminate the reaction, and the absorbance at 492 nm was monitored by a microplate reader (GENios Plus, Tecan).

LPS consists of lipid A and polysaccharides. Thus we tested whether rZRANB2 would bind to lipid A. A stock solution of lipid A purchased from Sigma was prepared by dissolving it in dimethyl sulfoxide, giving a concentration of 1 mg/ml. Aliquots of 50 μl of 80 μg/ml lipid A in 10 mM PBS, pH 7.4, were applied to each well of a 96-well microplate, air-dried in 25 °C, and processed as described above.

To test whether rZRANB2 has any lectin activity, aliquots of 50 μl of 80 μg/ml LPS in 10 mM PBS, pH 7.4, was applied to each well of a 96-well microplate and air-dried at 25 °C overnight. The plate was then incubated at 60 °C for 30 min to further fix the LPS, and the wells were each blocked with 200 μl of 1 mg/ml BSA in 10 mM PBS, pH 7.4, at 37 °C for 2 h. Meanwhile, aliquots of 50 μl of 3.5 μg/ml rZRANB2 or BSA (control) in 10 mM PBS, pH 7.4, containing different concentrations (0, 1.25, 2.5, 5, 10, and 20 mg/ml) of various sugars (D-glucose, D-mannose, D-galactose, GlcNAc, and *N*-acetyl-D-mannosamine) were preincubated at room temperature for 1 h and then added into each well. After incubation at room temperature for 3 h, the contents of each well were processed and measured as described above (49).

To examine whether rZRANB2 is able to bind to bacteria, aliquots of 150 μl of the Gram-negative bacteria *E. coli*, *Vibrio anguillarum*, and *Aeromonas hydrophila* and the Gram-positive bacteria *Staphylococcus aureus*, *Bacillus subtilis*, and *Micrococcus luteus* (1×10^8cells/ml) were mixed with 300 μl of 500 μg/ml rZRANB2 in 20 mM Tris-HCl buffer, pH 7.5, or with the same volume of Tris-HCl buffer alone (control). The mixtures were incubated at 25 °C for 2 h, and the bacteria were collected by centrifugation at 5000 × *g* at room temperature for 10 min. After washing with 20 mM Tris-HCl, the bacterial pellets were resuspended in 20 mM Tris-HCl, giving a concentration of 2×10^7 cells/ml. Both the rZRANB2-treated bacteria and the nontreated bacteria as well as purified rZRANB2 were run on a 12% SDS-PAGE followed by Western blotting analysis using rabbit anti-human ZRANB2 antibody as the primary antibody. The binding of rZRANB2 to the Gram-negative bacteria was also assayed by the method of Li *et al.* (50). In brief, *E. coli*, *V. anguillarum*, and *A. hydrophila* were mixed with rZRANB2 labeled with fluorescein isothiocyanate (FITC), and observed under an Olympus BX51 fluorescence microscope. For control, FITC-labeled BSA instead of rZRANB2 was used.

Assay for Antibacterial Activity of rZRANB2 in Vitro—The bacteria *E. coli* and *V. anguillarum* were cultured in LB medium at 37 °C to mid-logarithmic phase and collected by centrifugation at 6000 × *g* at room temperature for 10 min. Similarly, *A. hydrophila* was cultured in tryptic soy broth medium at 28 °C to mid-logarithmic phase and collected by centrifugation. The antibacterial activity of rZRANB2 against *E. coli* and *V. anguillarum* was assayed by the method of Yao *et al.* (51). To test the effect of Zn^{2+} on antibacterial activity, aliquots of 100 μl of rZRANB2 solution (50 μg/ml) were first mixed either with 1 μl of 1 mM $ZnCl_2$ plus 189 μl of the bacterial culture medium or with 1 μl of 100 mM EDTA (which is capable of chelating Zn^{2+}) plus 89 μl of the bacterial culture medium and then mixed with 10 μl of *E. coli* or *V. anguillarum* suspension (10^5 cells/ml). The positive and negative controls were processed similarly, except that rZRANB2 was replaced by kanamycin (2 μg/ml) or BSA (50 μg/ml). All of the mixtures were added to the wells of a 96-well plate and cultured at 37 °C. Inhibition of bacterial growth in each well was determined at each time point by measuring the absorbance at 600 nm with a Multiskan MK3 microplate reader every hour. The experiments were performed in triplicate and repeated three times.

A colony formation assay was used to test the antimicrobial activity of rZRANB2 against the Gram-negative bacterium *A. hydrophila* and the Gram-positive bacteria *S. aureus*, *B. subtilis*, and *M. luteus* (51). In brief, 100 μl of 10, 20, and 100 μg/ml rZRANB2 dissolved in 20 mM Tris-HCl buffer, pH 7.5, was mixed with 89 μl of the bacterial culture medium, 1 μl of 1 mM $ZnCl_2$, and 10 μl of an *A. hydrophila*, *S. aureus*, *B. subtilis*, or *M. luteus* suspension (8×10^4 cells/ml). To test the effect of

Zn^{2+} on antibacterial activity, 100 μl of 100 μg/ml rZRANB2 was first mixed either with 1 μl of 1 mM $ZnCl_2$ plus 189 μl of the bacterial culture medium or with 1 μl of 100 mM EDTA plus 89 μl of the bacterial culture medium and then mixed with 10 μl of an *A. hydrophila*, *S. aureus*, *B. subtilis*, or *M. luteus* suspension (10^5 cells/ml). The controls were processed similarly except that rZRANB2 was replaced by kanamycin and BSA. The mixtures were preincubated, with gentle stirring at 25 °C for 60 min and plated onto three agar plates (50 μl/plate). The percent of bacterial growth inhibition was calculated as follows: [number of colonies (control-test)/number of colonies (control)] $\times$100 ($n = 3$). The half-inhibitory concentration (IC_{50}) was defined as the lowest protein concentration at which the growth of the respective bacterium was 50% inhibited.

Flow Cytometry—Flow cytometry was used to measure the effect of rZRANB2 on the bacterial membranes of *E. coli*, *V. anguillarum*, and *A. hydrophila*. The culture and collection of the bacteria were as described above. After washing three times with PBS, pH 7.5, the bacterial pellets were suspended in PBS and adjusted to a density of 1×10^6 cells/ml, and then rZRANB2 was added to the bacterial suspensions, yielding final concentrations of 10 and 25 μg/ml for *E. coli* and 25 and 50 μg/ml for both *V. anguillarum* and *A. hydrophila*. In parallel, Triton X-100 and BSA were used instead of rZRANB2 for positive and negative controls. The mixtures were incubated at 28 °C for 2 h and fixed with 10 μM propidium iodide solution under dark conditions at 4 °C for 15 min. The bacterial cells stained by propidium iodide were examined using a FC500 MPL flow cytometer (Beckman). Data were analyzed using WinMDI, version 2.9, software (Scripps Research Inst., San Diego).

Assay for Antibacterial Activity of ZRANB2 in Embryos/Larvae—The 64–128-cell stage embryos of zebrafish were collected and washed three times with sterilized distilled water, homogenized, and centrifuged at 5000 $\times$ *g* at 4 °C for 10 min. As rZRANB2 showed conspicuous antibacterial activity against *E. coli*, *V. anguillarum*, and *A. hydrophila*, we wondered whether ZRANB2 would play any role in the immune defense in early embryos. First, we investigated the antibacterial activity of ZRANB2 in the embryo extracts. The antibacterial activity of the embryo extracts against *E. coli*, *V. anguillarum*, and *A. hydrophila* was assayed as described by Wang *et al.* (36). To precipitate ZRANB2 in the embryo extracts, 1 ml of the extracts was mixed with 0.5 μg of rabbit anti-human ZRANB2 antibody. For control, 1 ml of the embryo extracts was mixed with 0.5 μg of anti-β-actin antibody. Next, we assayed whether ZRANB2 had any ability to protect developing embryos *in vivo*. Fifty of the 8-cell stage embryos were dechorionated, microinjected into the yolk sac with 6 nl of sterilized PBS, pH 7.4 (blank control), anti-ZRANB2 antibody solution (0.33 ng), anti-actin antibody solution (0.33 ng), purified rZRANB2 solution (0.6 ng), or BSA solution (0.6 ng), and challenged 1 h later by injection of 6 nl of live *A. hydrophila* suspension (~500 cells). The mortality rate was recorded, and the cumulative mortality rate was calculated at 24 h after the bacterial injection. To confirm the specificity of the antimicrobial activity of rZRANB2 *in vivo*, anti-ZRANB2 antibody was injected together with rZRANB2 into the embryos, which were then challenged by injection of live *A. hydrophila* (29). For control, the embryos were co-injected with anti-actin antibody and rZRANB2 and treated similarly.

To verify the killing of *A. hydrophila* by developing embryos, 8-cell stage embryos were dechorionated and microinjected with live *A. hydrophila* as described above. Five embryos were collected each time at 0, 12, and 24 h after the bacterial injection. The normal embryos were similarly collected as controls. The total DNAs were isolated from each embryo according to the method of Wang *et al.* (36) and used for PCR and qRT-PCR analyses. PCR and qRT-PCR were carried out, respectively, to amplify a specific region of the *A. hydrophila* 16s rRNA gene using the sense primer 16s rRNAS 5-AATACCGCATACGCCCTAC-3, antisense primer 16s rRNAA 5-AACCCAACATCTCACGACAC-3, sense primer q16s rRNAS GTAAAGGCCTACCATGGCGACGATC, and antisense primer q16s rRNAA GCCGGTGCTTATTCTGCAGCTAATG (Table 1), which were designed on the basis of the *A. hydrophila* 16s rRNA sequence (GenBank™ accession number DQ207728).

Titration of ZRANB2 Content in Eggs and Embryos—Exactly 120 embryos were collected at 0, 12, and 24 hpf, washed three times with sterilized 0.9% saline, homogenized, and centrifuged at 5000 $\times$ *g* at 4 °C for 5 min. The supernatants were pooled and used to measure the contents of ZRANB2 in the extracts by ELISA using rabbit anti-human ZRANB2 antibody. In brief, 200 μl of rabbit anti-human ZRANB2 antibody diluted at 1:2500 with 10 mM PBS, pH 7.4, was applied to each well of a 96-well microplate at 4 °C overnight. After washing three times with 200 μl of PBS supplemented with 0.5% Tween 20, 200 μl of the embryo extracts or rZRANB2 (0, 5, 10, 25, 50, 100, and 200 ng/ml) was added to each well and detected as above. The mean diameter of zebrafish eggs measured was 600 μm, and therefore each egg/embryo volume was $\sim 1.1 \times 10^{-5}$ cm^3. Accordingly, the content of ZRANB2 in each egg/embryo was inferred as described by Liang *et al.* (52).

Structure-Activity Assays—To determine the structure-activity relationship, N-terminal deletion of ZRANB2 was carried out. The cDNA region encoding the C-terminal 161 residues 38–198 ($Z_{38/198}$; with the N-terminal 37 residues depleted) of ZRANB2 was amplified by PCR using the sense primer z38/198S (BamHI site is underlined) and the antisense primer z38/198A (HindIII site is underlined) (Table 1). Construction of the expression vector plasmid *pET28a/z38/198* and its transformation into *E. coli* BL21 were performed as described above. The *E. coli* BL21 with *pET28a/z38/198* was cultured in LB broth containing 50 μg/ml kanamycin overnight. The culture was diluted 1:100 with LB broth and subjected to further incubation until A_{600} reached about 1.0 at 37 °C. The expression of $rZ_{38/198}$ was induced by adding isopropyl 1-thio-β-D-galactopyranoside to the culture at a final concentration of 0.1 mM, and then the culture was incubated at 28 °C for about 12 h. The protein $rZ_{38/198}$ was then purified and characterized. The antibacterial activity of $Z_{38/198}$ against *E. coli*, *V. anguillarum*, and *A. hydrophila* and its affinity to LPS were assayed as described above. As the polypeptide $Z_{38/198}$ lost nearly all antibacterial activity (see below), thus two peptides (purity > 99%) comprising the N-terminal 37 residues ($Z_{1/37}$) and the N-terminal 26 residues ($Z_{11/37}$, which consists of the ZnF_RBZ domain *per se*) of ZRANB2 were synthesized by Sangon Biotech (Shanghai, China) and

TABLE 1
Sequences of the primers used in this study
Restriction enzyme sites are underlined.

Primers	Sequences (5′-3′)
For *zranb2* cloning	
zranb2S (sense)	TGTCGGGGAAGAGTTTTCGCGTTAG
zranb2A (antisense)	GACCGGGAACTTGGACAAATCTGCA
For qRT-PCR	
qzranb2S (sense)	TTCGTGGGAAAACCAAGAAGGATAG
qzranb2A (antisense)	CTGCATCATCTTCATCATCATCATC
β-ActinS (sense)	GATGCGGAAACTGGAAAGGG
β-ActinA (antisense)	AGGAGGGCAAAGTGGTAAACG
For WISH-PCR	
wzranb2S (sense)	TCGGGGAAGAGTTTTCGCGTT
wzranb2A (antisense)	AGACCGGGAACTTGGACAAATCTGC
For ZRANB2 expression *in vitro*	
rzranb2S (sense)	GCGGATCCTCGGGGAAGAGTTTTCGCGTT
rzranb2A (antisense)	GCCAAGCTTGACCGGGAACTTGGACAAATCTGCA
For $Z_{38/198}$ expression *in vitro*	
z38/198S (sense)	GCGGATCCAAGACGACTGAAGCAAAGATGATG
z38/198A (antisense)	GCCAAGCTTGACCGGGAACTTGGACAAATCTGCA
For 16s rRNA of *A. hydrophila*	
16s rRNAS (sense)	AACCCAACATCTCACGACAC
16s rRNAA (antisense)	AATACCGCATACGCCCTAC
For qRT-PCR of 16s rRNA of *A. hydrophila*	
q16s rRNAS (sense)	GCCGGTGCTTATTCTGCAGCTAATG
q16s rRNAA (antisense)	GCCGGTGCTTATTCTGCAGCTAATG

TABLE 2
Names and accession numbers of ZRANB2 proteins

Name	Abbreviation	Accession No.
Homo sapiens ZRANB2 isoform 1	Hs1ZRANB2	NP_976225.1
Homo sapiens ZRANB2 isoform 2	Hs2ZRANB2	NP_005446.2
Bos Taurus ZRANB2	BZRANB2	AAI34560.1
Mus musculus ZRANB2	MZRANB2	NP_059077.1
Ovis aries ZRANB2 isoform 1	Os1ZRANB2	XP_004002129.1
Ovis aries ZRANB2 isoform 2	Os2ZRANB2	XP_004002129.2
Gorilla gorilla gorilla ZRANB2 isoform 1	Gs1ZRANB2	XP_004026019.1
Gorilla gorilla gorilla ZRANB2 isoform 2	Gs2ZRANB2	XP_004026020.1
Gallus gallus ZRANB2	GZRANB2	NP_001026468.1
Orcinus orca ZRANB2 isoform 1	Ors1ZRANB2	XP_004280780.1
Orcinus orca ZRANB2 isoform 2	Ors2ZRANB2	XP_004280781.1
Xenopus tropicalis ZRANB2	XZRANB2	NP_001136134.1
Takifugu rubripes ZRANB2-like isoform 2	TaZRANB2	NC_018909.1
Tetraodon nigroviridis ZRANB2	TeZRANB2	CAG01185.1
Danio rerio ZRANB2	DZRANB2	NP_998572.1

subjected to antibacterial activity and LPS binding assays. For the antibacterial activity assay of $Z_{1/37}$ and $Z_{11/37}$, LPS was biotinylated with NHS-LC-biotin instead of the peptides because of the small molecular mass. $Z_{38/198}$, $Z_{1/37}$, and $Z_{11/37}$ were also microinjected into zebrafish embryos followed by challenge of live *A. hydrophila*, as described above, to test their bioactivity *in vivo*.

Statistical Analysis—All of the experiments were conducted at least three times. Statistical analyses were performed using GraphPad Prism 5. The significance of difference was determined by one-way analysis of variance. The difference at $p < 0.05$ was considered significant. All of the data were expressed as mean ± S.D.

Results

ZRANB2 Is a LPS-binding Protein Stored in Early Embryos—The proteins eluted from the LPS-conjugated Sepharose CL-4B column were resolved by SDS-PAGE and silver-stained, and we identified two main bands (*a* and *b*) of ~38.9 and 22.7 kDa (Fig. 1*a*). MALDI/TOF MS analysis revealed that band *a* was ZNF365, consisting of 345 amino acids (data not shown), and band *b* was zinc finger Ran-binding domain (ZnF_RBZ)-containing protein 2, ZRANB2 (GenBank™ accession number AAH52752.1) consisting of 198 amino acids (Fig. 1*b*).

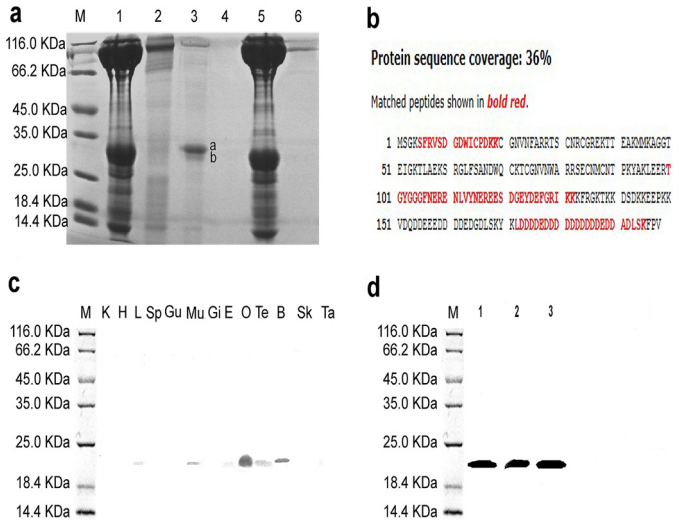

FIGURE 1. **Identification of ZRANB2 as an LPS-binding protein, including SDS-PAGE results, protein sequence, and Western blotting analysis of ZRANB2 in the different tissues and embryo extracts.** *a*, SDS-PAGE of the proteins isolated from the embryos extracts of zebrafish on LPS-conjugated Sepharose CL-4B affinity resin. *Lane M*, marker; *lane 1*, embryos extracts; *lane 2*, effluent fractions after Tris-HCl washing; *lane 3*, effluent fractions containing the adsorbed proteins *a* and *b*; *lane 4*, effluent fractions when all proteins were washed clean; *lane 5*, positive control, effluent fractions from Sepharose CL-4B affinity resin without LPS; *lane 6*, negative control, effluent fractions from LPS-Sepharose CL-4B affinity resin but with no embryos extracts loaded. *b*, the protein sequence. The matched peptides are shown in *red*. *c*, Western blotting analysis of ZRANB2 in the different tissues including kidney (*K*), heart (*H*), liver (*L*), spleen (*Sp*), gut (*Gu*), muscle (*Mu*), gill (*Gi*), eye (*E*), ovary (*O*), testis (*Te*), brain (*B*), skin (*Sk*), and tail (*Ta*). *d*, Western blotting analysis of the embryo extract after 0 h (*lane 1*), 12 h (*lane 2*), and 24 h (*lane 3*) post-fertilization.

Western blotting showed that ZRANB2 was primarily present in the liver, muscle, eye, brain, ovary, and testis, with the level in the ovary being highest (Fig. 1*c*), suggesting that ZRANB2 was distributed mainly in the ovary. Accordingly, ZRANB2 was also detected in the fertilized eggs and the 12- and 24-h embryos (Fig. 1*d*). These data suggest that ZRANB2 is a LPS-binding protein stored maternally in the eggs/embryos of zebrafish.

ZRANB2 Is Localized in Cytoplasm—Immunohistochemical examination showed that ZRANB2 was localized predominantly in the blastoderm in 4-, 8-, 32-, and 128-cell stage embryos and in the epidermis and neural tube in the head of 24-hpf larvae, with little positive signal (green fluorescence) in the yolk sac (Fig. 2, *a* and *b*, *B* and *C*). In the 6-hpf embryos, ZRANB2 was clearly found to be distributed in the cytoplasm (Fig. 2*bA*), indicating that ZRANB2 is a protein localized in the cytoplasm of embryonic cells.

Structure, Phylogenetics, and Synteny of zranb2—Zebrafish ZRANB2 cDNA obtained was 2044-bp long and contained an open reading frame of 597 bp coding for a protein of 198 amino acids with a calculated molecular mass of ~22.7 kDa and a pI of 4.36, a 5′-untranslated region of 63 bp, and a 3′-untranslated region of 166 bp (supplemental Fig. S1). Zebrafish ZRANB2 has eight highly conserved cysteine residues spaced appropriately to give rise to two ZnF_RBZ domains (at residues 1–40 and 65–95; Fig. 3*a*) as well as the motifs N*XXF*X*RR*X*XX*N and N*XX*-

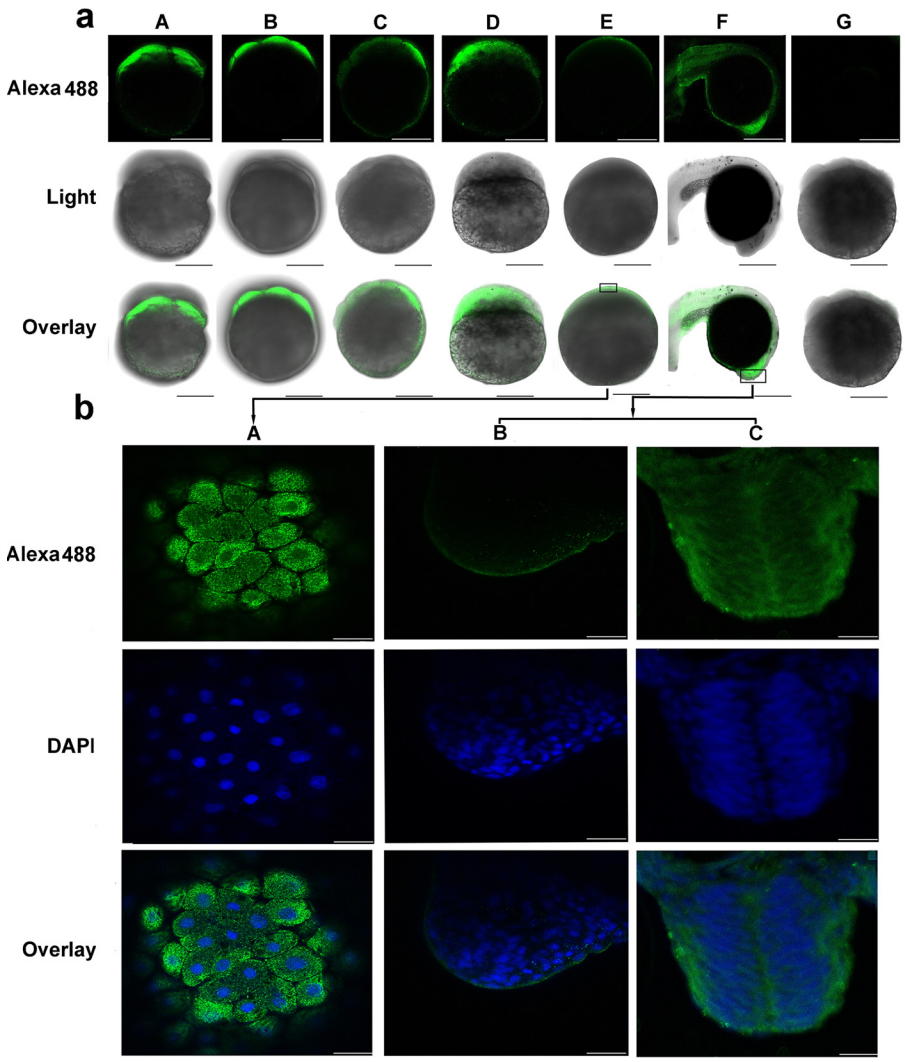

FIGURE 2. **Distribution of ZRANB2 in the different developmental stage embryos of zebrafish observed under confocal microscope.** *a*, embryos at different development stages: *A*, 4-cell stage; *B*, 8-cell stage; *C*, 32-cell stage; *D*, 128-cell stage; *E*, 6-hpf embryo; *F*, 24-hpf embryo; *G*, 8-cell embryo incubated with rabbit preimmune serum as a negative control. Nuclei were visualized by DAPI staining (*blue*). *Scale bars* represent 250 μm. *b*, high resolution of *panels* in *a*: *A*, high resolution of *aE*; *B*, high resolution of *aF*; *C*, high resolution of a frozen section of view shown in *aF*. *Scale bars* in *A* and *B* represent 10 μm, and *scale bars* in *C* represent 25 μm.

W*X*RR*XXX*N of the RNA-binding region (supplemental Fig. S2), characteristic of known ZRANB2 proteins, but it lacks the typical nuclear localization signal (supplemental Table S1) and the C-terminal serine-rich domain (supplemental Fig. S2). Sequence alignment showed that zebrafish ZRANB2 was 79.2%, 80.3%, 80.6%, and 82.3% identical to mammalian, avian, amphibian, and teleost ZRANB2 at amino acid levels (supplemental Fig. S3). The structure prediction using the SWISS-MODEL online software revealed that the three-dimensional structures of the ZnF_RBZ domains of both zebrafish and human ZRANB2 consist mainly of β-sheets (Fig. 3*b*). The first ZnF_RBZ domains (at residues 1–40) of zebrafish and human ZRANB2 share a similar three-dimensional structure with a Zn^{2+}-binding site, whereas the second ZnF_RBZ domain (at residues 65–95) of zebrafish and human ZRANB2 are different in that the second ZnF_RBZ domain of zebrafish ZRANB2 has no Zn^{2+}-binding site (Fig. 3*b*).

The phylogenetic tree constructed using the available sequences of ZRANB2 proteins shows that zebrafish ZRANB2 is grouped together with other teleost ZRANB2 forming an independent clade branched from mammalian, avian, and amphibian counterparts. This well reflects the established phylogeny of chosen organisms. Syntenic analysis showed that zebrafish *zranb2* is mapped onto chromosome 6 and closely linked to *Negr1* and *Ptger*, which is similar to human, cow, mouse, and frog *zranb2* (Fig. 3*d*). Additionally, the direction of zebrafish *zranb2* relative to *Negr1* and *Ptger* is comparable with that of human, cow, mouse, and frog *zranb2* (Fig. 3*d*), implying that the linkage of *zranb2* with *Negr1* and *Ptger* is conserved from fish to humans.

Tissue- and Stage-specific Expression of zranb2—qRT-PCR showed that *zranb2* is expressed primarily in the liver, muscle, eye, brain, ovary, and testis in a tissue-specific manner, with the most abundant expression in the ovary (Fig. 4*a*), consistent with the tissue-specific distribution of ZRANB2 (Fig. 1, *c* and *d*). As shown in Fig. 4*b*, *zranb2* mRNA was abundant in the zygotes (0 hpf) but decreased continuously as development went forward, and from 15 hpf onward

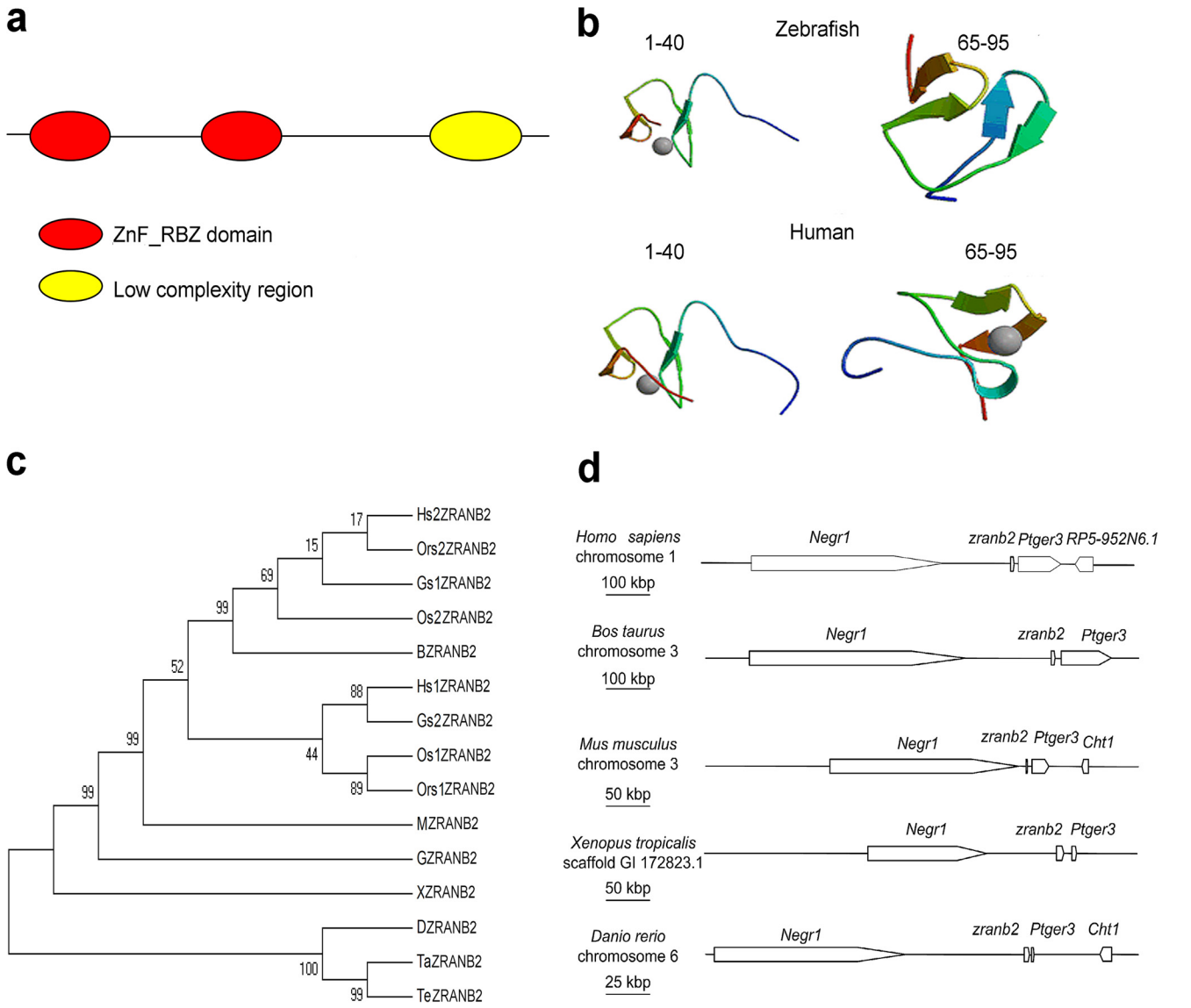

FIGURE 3. **Structure, phylogenetics, and synteny of ZRANB2 of zebrafish.** *a*, domain structure of ZRANB2 predicted by the SMART program. *b*, three-dimensional structure of ZRANB2 generated by SWISS-MODEL online software using residues 1–40 (PDB code: 1n0z.1.A) and residues 65–95 (PDB code: 2k1p.1.A) of human ZRANB2 as the model. *Gray balls* indicate Zn^{2+}. *c*, phylogenetic tree constructed by MEGA, version 4.1, using the neighbor-joining method. The reliability of each node was estimated by bootstrapping with 1000 replications. The *numbers* shown at each node indicate the bootstrap values (%). The accession numbers of ZRANB2 proteins used are listed in Table 2. *d*, syntenic map of the genomic segment where *zranb2* resides in the chromosomes of zebrafish and other vertebrates including humans. *Boxes* represent the genes; *Ptger3* is linked with *zranb2*. The direction of box represents the direction of gene.

only slight mRNA was detected in the embryos/larvae. These findings indicate that the maternal *zranb2* mRNA level is relatively higher in the fertilized eggs, which decreases with development.

As shown in Fig. 4*c*, pan-expression of *zranb2* was observed in the embryos before segmentation stages (Fig. 4*c*, *A–D*), and then *zranb2* mRNA was observed primarily in the head of 1- and 2-day-old larvae (Fig. 4*c*, *E* and *F*), which have the brain and eyes as the main organs in the head at this stage; but little signal was detected in 3- and 5-day-old larvae (Fig. 4*c*, *G* and *H*). This is basically consistent with the distribution of ZRANB2 protein in the embryos (Fig. 2). These findings suggest that ZRANB2 may play a role in early development, especially in the formation of the head including the brain and eyes.

rZRANB2 Interacts with LPS, Lipid A, and Gram-negative Bacteria—Zebrafish ZRANB2 was expressed in *E. coli* BL21 (DE3) and purified by affinity chromatography on a nickel-nitrilotriacetic acid resin column. The purified recombinant protein, rZRANB2, yielded a single band of ~27.6 kDa on SDS-PAGE after Coomassie Blue staining, corresponding to the expected size (Fig. 5*a*). Western blotting analysis showed that the purified protein reacted with the rabbit anti-human ZRANB2 antibody, indicating that rZRANB2 was correctly expressed (Fig. 5*b*).

As shown in Fig. 5*c*, rZRANB2 interacted with LPS in a dose-dependent manner, whereas BSA used as negative control did not, confirming without a doubt that zebrafish ZRANB2 is indeed a LPS-binding protein. We then tested for whether rZRANB2 binds to lipid A, a core component of LPS. It was

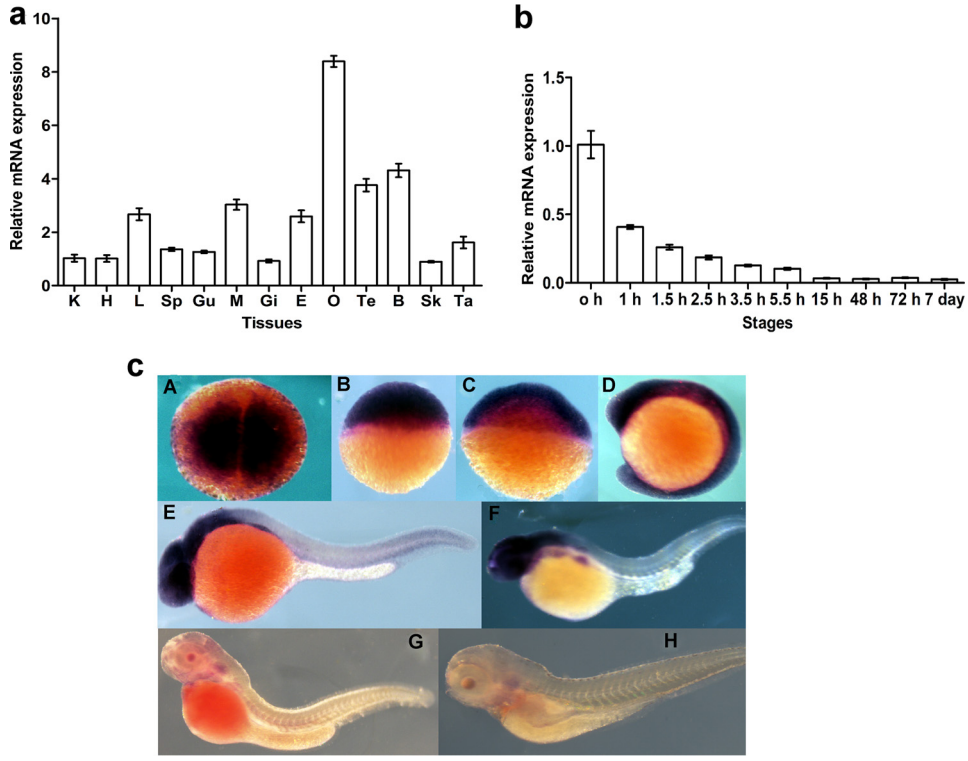

FIGURE 4. **Expression patterns of zebrafish *zranb2* in the different tissues and at the different developmental stages.** *a*, expression profiles of zebrafish *zranb2* in the different tissues including kidney (*K*), heart (*H*), liver (*L*), spleen (*Sp*), gut (*Gu*), muscle (*Mu*), gill (*Gi*), eye (*E*), ovary (*O*), testis (*Te*), brain (*B*), skin (*Sk*), and tail (*Ta*). *b*, expression profiles of zebrafish *zranb2* at the different developmental stages including zygote (0 h), 4-cell stage (about 1 h), 16-cell stage (~1.5 h), 256-cell stage (~2.5 h), high blastula stage (~3.5 h), 50% epiboly stage (~5.5 h), 10-somite stage (~15 h), 2 day post-fertilization (2 dpf), 3 dpf, and 7 dpf. β-Actin was chosen as the internal control for normalization. Relative expression data were calculated by the method of $2^{-\Delta\Delta Ct}$. The *vertical bars* represent the mean ± S.D. ($n = 3$). The data are from three independent experiments performed in triplicate. *c*, expression of *zranb2* during early development detected by WISH. Stages of embryonic development: 2-cell stage (~0.75 h), 256-cell stage (~2.5 h), 50% epiboly stage (~5 h), 10-somite stage (~15 h), 1 dpf, 2 dpf, 3 dpf, and 5 dpf.

found that rZRANB2 displayed an affinity to lipid A comparable with that of LPS (Fig. 5*d*), which agrees with the observations that zinc finger proteins have lipid binding activity (53, 54). Interestingly, the affinity of rZRANB2 to LPS was not inhibited by any of the sugars examined, even at a concentration as high as 20 mg/ml (Fig. 5*e*). Notably, the optical density of BSA in Fig. 5*e* was slightly higher than that in Fig. 5, *c* and *d*. This superficial increase in OD value resulted from the difference in coloration time. The coloration time was about 10 min in Fig. 5, *c* and *d*, whereas in Fig. 5*e*, the coloration time was extended to 30 min, thus leading to a deeper color and a greater OD value. Altogether, these findings indicate that rZRANB2 has little lectin activity. It is clear that zebrafish ZRANB2 may bind to LPS via lipid A.

Western blotting showed that rZRANB2 also bound to *E. coli*, *V. anguillarum* and *A. hydrophila* (Fig. 5*f*). In addition, FITC-labeled rZRANB2 exhibited affinity to all of the Gram-negative bacteria tested (Fig. 5*g*). By contrast, rZRANB2 could not bind to the Gram-positive bacteria *S. aureus*, *B. subtilis*, or *M. luteus* (supplemental Fig. S4). These findings suggest that zebrafish rZRANB2 interacts only with Gram-negative bacteria, further strengthening the idea that ZRANB2 is a LPS-binding protein.

Bactericidal Activity of rZRANB2—As zebrafish ZRANB2 is a LPS-binding protein, we thus wanted to know whether it has antibacterial activity. As shown in Fig. 6, the growth of the Gram-negative bacteria *E. coli*, *V. anguillarum*, and *A. hydrophila* was inhibited by rZRANB2 in a dose-dependent manner when Zn^{2+} was present (Figs. 6, *a–c*, and 9*a*), indicating that in addition to the LPS binding activity, rZRANB2 can also inhibit Gram-negative bacterial growth. When the concentration of rZRANB2 was at 10 μg/ml or above, the growth of all the Gram-negative bacteria tested was significantly suppressed. By contrast, removal of Zn^{2+} completely abolished the antibacterial activity of rZRANB2 against *E. coli*, *V. anguillarum*, and *A. hydrophila*, suggesting the dependence of antibacterial activity of rZRANB2 upon Zn^{2+} (Fig. 6, *a–c*). It was also shown that rZRANB2 did not inhibit the growth of the Gram-positive bacteria *S. aureus*, *B. subtilis*, and *M. luteus* even in the presence of Zn^{2+} (supplemental Fig. S4), suggesting that ZRANB2 can specifically inhibit the growth of Gram-negative bacteria but not Gram-positive bacteria.

Flow cytometry revealed that a few of the *E. coli*, *V. anguillarum*, and *A. hydrophila* cells treated with BSA, or non-treated, showed a propidium iodide fluorescent signal (Fig. 6*d*), indicating that they had intact and viable cell membranes. By contrast, a significant proportion of the *E. coli*, *V. anguillarum*, and *A. hydrophila* cells treated with rZRANB2 displayed a fluorescent signal, and the number of cells with a fluorescent signal increased with increasing doses of rZRANB2, indicating that their cell membranes were no longer intact and became permeable to propidium iodide. These findings suggest that

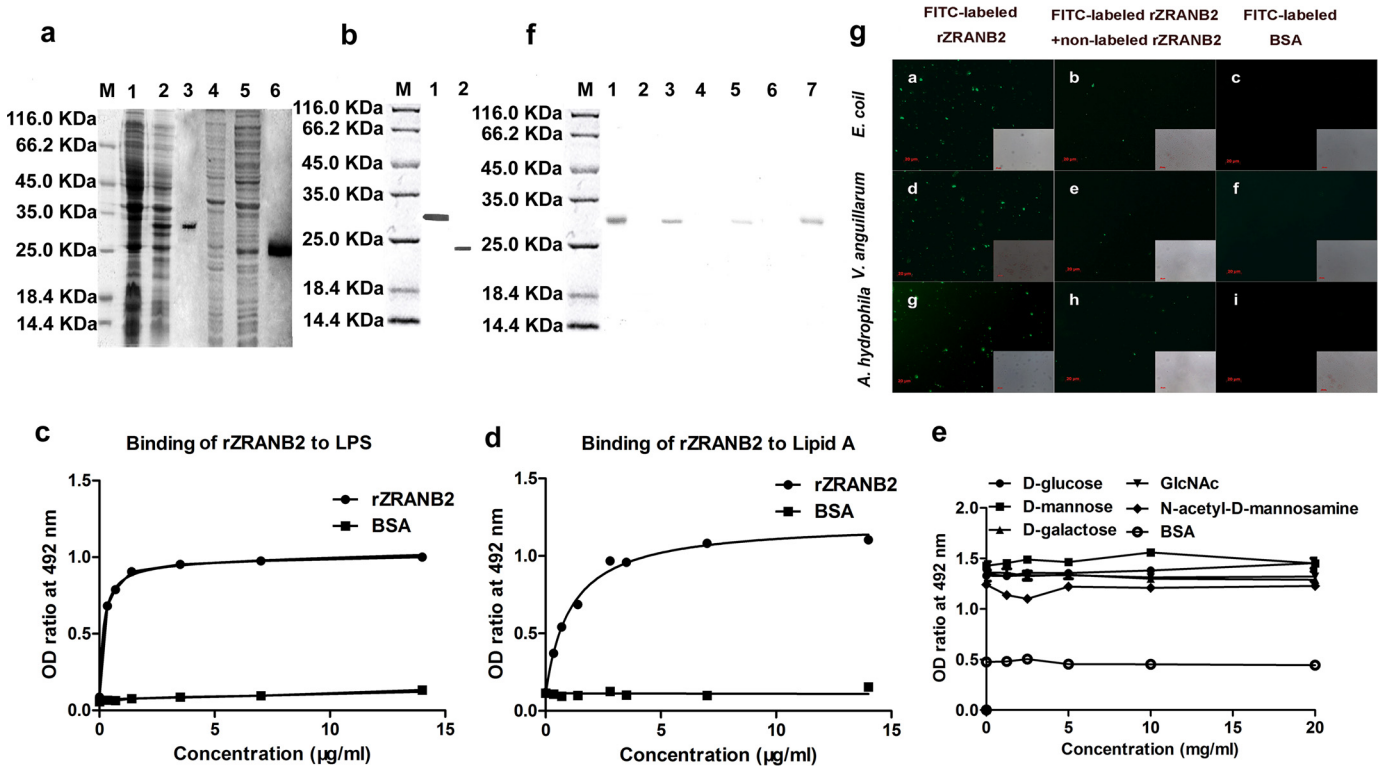

FIGURE 5. **SDS-PAGE, Western blotting analysis, and binding of rZRANB2 to LPS, lipid A, and bacteria.** *a*, SDS-PAGE of recombinant proteins rZRANB2 and $Z_{38/198}$. *Lane M*, molecular mass standards; *lane 1*, total cellular extracts from *E. coli* BL21 containing expression vector *pET28a/zranb2* before induction; *lane 2*, total cellular extracts from isopropyl 1-thio-β-D-galactopyranoside-induced *E. coli* BL21 containing expression vector *pET28a/zranb2*; *lane 3*, rZRANB2 purified on Ni-NTA resin column; *lane 4*, total cellular extracts from *E. coli* BL21 containing expression vector *pET28a/*$Z_{38/198}$ before induction; *lane 5*, total cellular extracts from isopropyl 1-thio-β-D-galactopyranoside-induced *E. coli* BL21 containing expression vector *pET28a/*$Z_{38/198}$; *lane 6*, $Z_{38/198}$ purified on Ni-NTA resin column. *b*, Western blotting of recombinant proteins rZRANB2 and $Z_{38/198}$. *Lane 1*, rZRANB2 of Western blotting analysis; *lane 2*, $Z_{38/198}$ of Western blotting analysis. *c*, interaction of rZRANB2 with LPS. Wells coated with LPS were incubated with different concentrations of rZRANB2. BSA was used instead of rZRANB2 as a negative control. Both rZRANB2 and BSA were biotinylated individually with biotinamidohexanoic acid *N*-hydroxysuccinimide ester. The binding of rZRANB2 was detected using streptavidin-HRP. Each point in the graph represents the mean ± S.D. ($n = 3$). The data are from three independent experiments performed in triplicate. The *bars* represent the mean ± S.D. *d*, interaction of rZRANB2 with lipid A. Wells coated with lipid A were incubated with different concentrations of rZRANB2. BSA was used as the control. Both rZRANB2 and BSA were biotinylated individually with biotinamidohexanoic acid *N*-hydroxysuccinimide ester. The binding of rZRANB2 was detected using streptavidin-HRP. Each point in the graph represents the mean ± S.D. ($n = 3$). The data are from three independent experiments performed in triplicate. The *bars* represent the mean ± S.D. *e*, effect of various sugars on the interaction of rZRANB2 with LPS. Wells were coated with LPS. rZRANB2 preincubated with different concentrations of sugars (0, 1.25, 2.5, 5, 10, and 20 mg/ml) was added to each well and incubated at room temperature for 3 h. BSA was used as a control. Both rZRANB2 and BSA were biotinylated individually with biotinamidohexanoic acid *N*-hydroxysuccinimide ester. The binding of rZRANB2 was detected using streptavidin-HRP. Each point in the graph represents the mean ± S.D. ($n = 3$). The data are from three independent experiments performed in triplicate. The *bars* represent the mean ± S.D. *f*, Western blotting about interaction of rZRANB2 with microbes. *Lane M*, marker; *lane 1*, purified rZRANB2; *lanes 2*, *4*, and *6*, *E. coli*, *V. anguillarum*, and *A. hydrophila* incubated in the absence of rZRANB2; *lanes 3*, *5*, and *7*, *E. coli*, *V. anguillarum*, and *A. hydrophila* incubated in the presence of rZRANB2. *g*, binding of FITC-labeled rZRANB2 to microbial cells: *A*, *D*, and *G*, binding of FITC-labeled rZNRANB2 to *E. coli*, *V. anguillarum*, and *A. hydrophila*; *B*, *E*, and *H*, binding of FITC-labeled rZRANB2 and non-labeled rZRANB2 to *E. coli*, *V. anguillarum*, and *A. hydrophila*; *C*, *F*, and *I*, no binding of FITC-labeled BSA to *E. coli*, *V. anguillarum*, or *A. hydrophila*. *Scale bars* represent 20 μm.

rZRANB2 is able to destroy the membrane integrity of *E. coli*, *V. anguillarum*, and *A. hydrophila* cells.

ZRANB2 Is Involved in Antibacterial Defense of Early Embryos—The protein concentration of the extracts prepared from 64–128-cell stage embryos was ~5 mg/ml. The embryo extracts showed conspicuous antimicrobial activity against *E. coli*, *V. anguillarum*, and *A. hydrophila*; this bacterial growth-inhibitory activity was significantly reduced by preincubation of the extracts with anti-human ZRANB2 antibody but not by preincubation with anti-actin antibody (Fig. 7, *a–c*). These findings suggest that ZRANB2 in the embryo extracts is a molecule capable of inhibiting bacterial growth.

To examine whether ZRANB2 plays the same role *in vivo*, 8-cell stage embryos were each microinjected with anti-ZRANB2 antibody to block ZRANB2 action followed by injection with live *A. hydrophila* (pathogenic to *D. rerio*). The majority (~94%) of the embryos injected with PBS, BSA, anti-actin antibody, anti-ZRANB2 antibody, rZRANB2, rZRANB2 plus anti-actin antibody, or rZRANB2 plus anti-ZRANB2 antibody developed normally, with the 24-h cumulative mortality rate being about 6% (Fig. 7*d*). Notably, the challenge with live *A. hydrophila* resulted in a significant increase in the mortality rate of the embryos injected with anti-ZRANB2 antibody (resulting in a decrease of ZRANB2), with a 24-h mortality rate of ~85.7%, whereas the same challenge caused only ~64.3, 65.0, and 66.0% mortality at 24 h in the embryos injected with either anti-actin antibody or BSA or PBS alone (Fig. 7*d*), indicating that blocking of ZRANB2 action in the embryos was able to reduce their anti-*A. hydrophila* activity. In comparison, the 24-h mortality rate of the embryos injected with rZRANB2 (resulting in an increase of ZRANB2) was reduced to ~53.3%, which is markedly lower than that of the embryos injected with

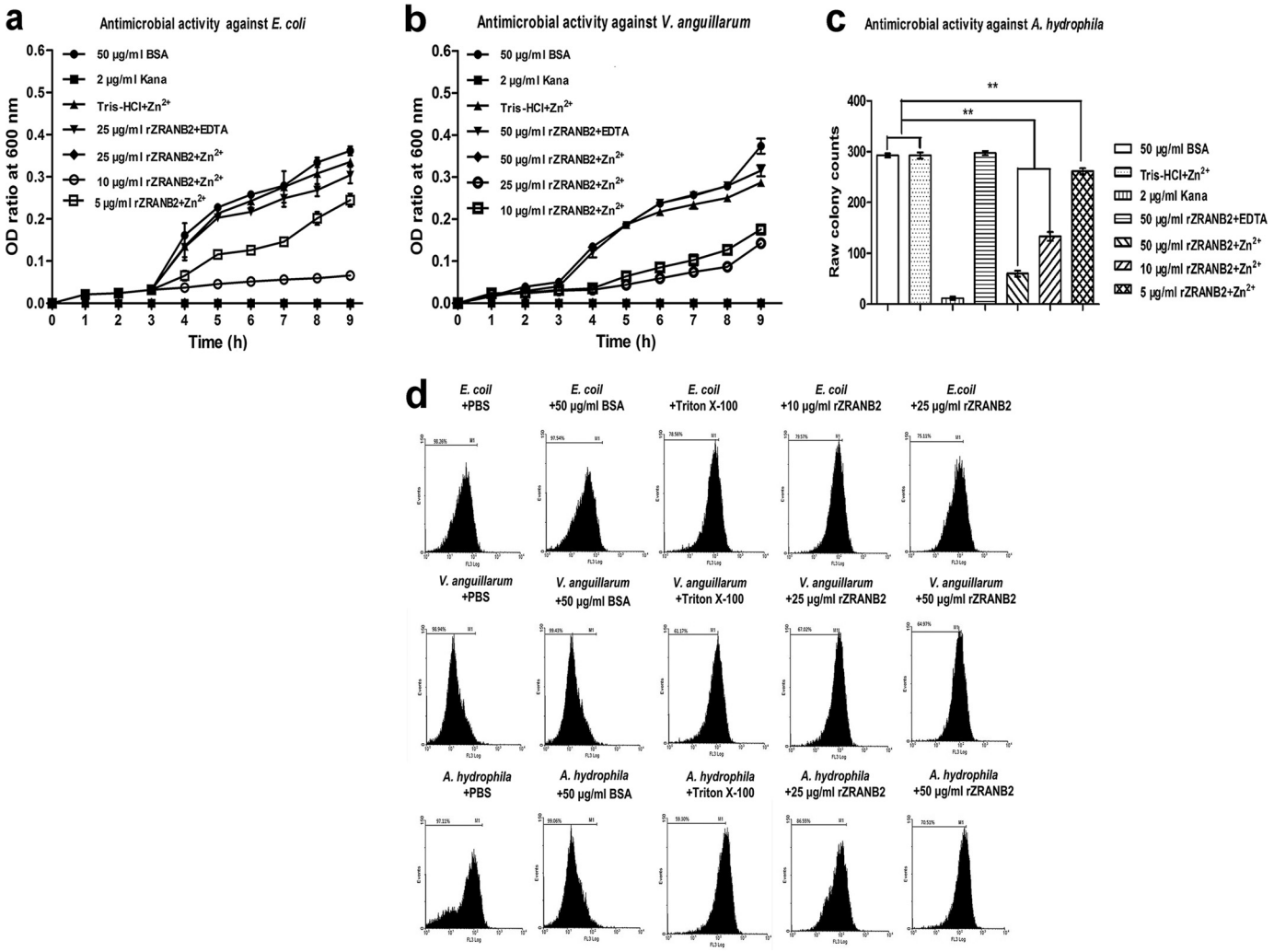

FIGURE 6. **The bactericidal activity of rZRANB2 against *E. coli*, *V. anguillarum*, and *A. hydrophila*.** *a*, antibacterial activity of rZRANB2 against *E. coli*. *b*, antibacterial activity of rZRANB2 against *V. anguillarum*. *c*, antibacterial activity of rZRANB2 against *A. hydrophila*. Each point in the graph represents the mean ± S.D. ($n = 3$). The data are from three independent experiments performed in triplicate. The *bars* represent the mean ± S.D. **, extremely significant difference ($p < 0.01$). *d*, effects of rZRANB2 on the membrane integrity of *E. coli*, *V. anguillarum*, and *A. hydrophila* cells analyzed by flow cytometry. The proportion of integrated cells is shown near the marker (*M1*).

anti-actin antibody or BSA or PBS alone, suggesting that the increased amount of ZRANB2 contributed to the protection of embryos against *A. hydrophila* attack. Moreover, the embryo protecting activity of rZRANB2 was apparently reduced by co-injection of anti-ZRANB2 antibody but not by co-injection of anti-actin antibody (24-h mortality rate being ~84.3 *versus* ~52.3%), thus implying the specificity of ZRANB2 antibacterial activity. All of these data suggest that ZRANB2 is involved in the antimicrobial defense of early embryos of zebrafish.

To prove the killing of live *A. hydrophila* by the embryos, both PCR and qRT-PCR were performed to amplify a specific region of the *A. hydrophila* 16s rRNA gene. As shown in Fig. 7*e*, no band was observed in the control sample (from embryos without injected *A. hydrophila*), but intense bands were found in the embryos collected soon after the bacterial injection (0 h). The band intensities apparently decreased with time (at 12 and 24 h), suggesting the lysis of the bacterium by the embryos (Fig. 7, *eA*). Similarly, the microinjection of anti-actin antibody into the embryos also failed to suppress the reduction of the band intensity at 12 and 24 h, *i.e. A. hydrophila* lysis continued in the embryos (Fig. 7, *eB*). By contrast, the injection of anti-ZRANB2 antibody into the embryos clearly suppressed the decrease in the band intensity during the initial 12 and 24 h (Fig. 7, *eC*), *i.e.* little *A. hydrophila* lysis took place in the embryos. This was further supported by the results of qRT-PCR (Fig. 7*f*), which showed that expression of the 16s rRNA gene of *A. hydrophila* in the embryos injected with anti-actin antibody decreased significantly ($p < 0.5$), but its expression in the embryos injected with anti-ZRANB2 antibody did not ($p > 0.5$). These data suggest a clear correlation between ZRANB2 content and lysis of the bacterium in the early embryos.

ELISA analysis revealed that the concentrations of ZRANB2 in each of the newly fertilized eggs as well as in each of the 12- and 24-h embryos were about 10.0, 14.2, and 20.1 μg/ml, respectively. The increase of ZRANB2 in the 12- and 24-h embryos may be due to the translation of ZRANB2 mRNA stored in eggs during embryogenesis (Fig. 4*b*). rZRANB2 was able to significantly inhibit the growth of all the Gram-negative bacteria tested at a concentration of 10 μg/ml or above (Fig. 6, *a–c*), and thus the endogenous concentration of ZRANB2 in

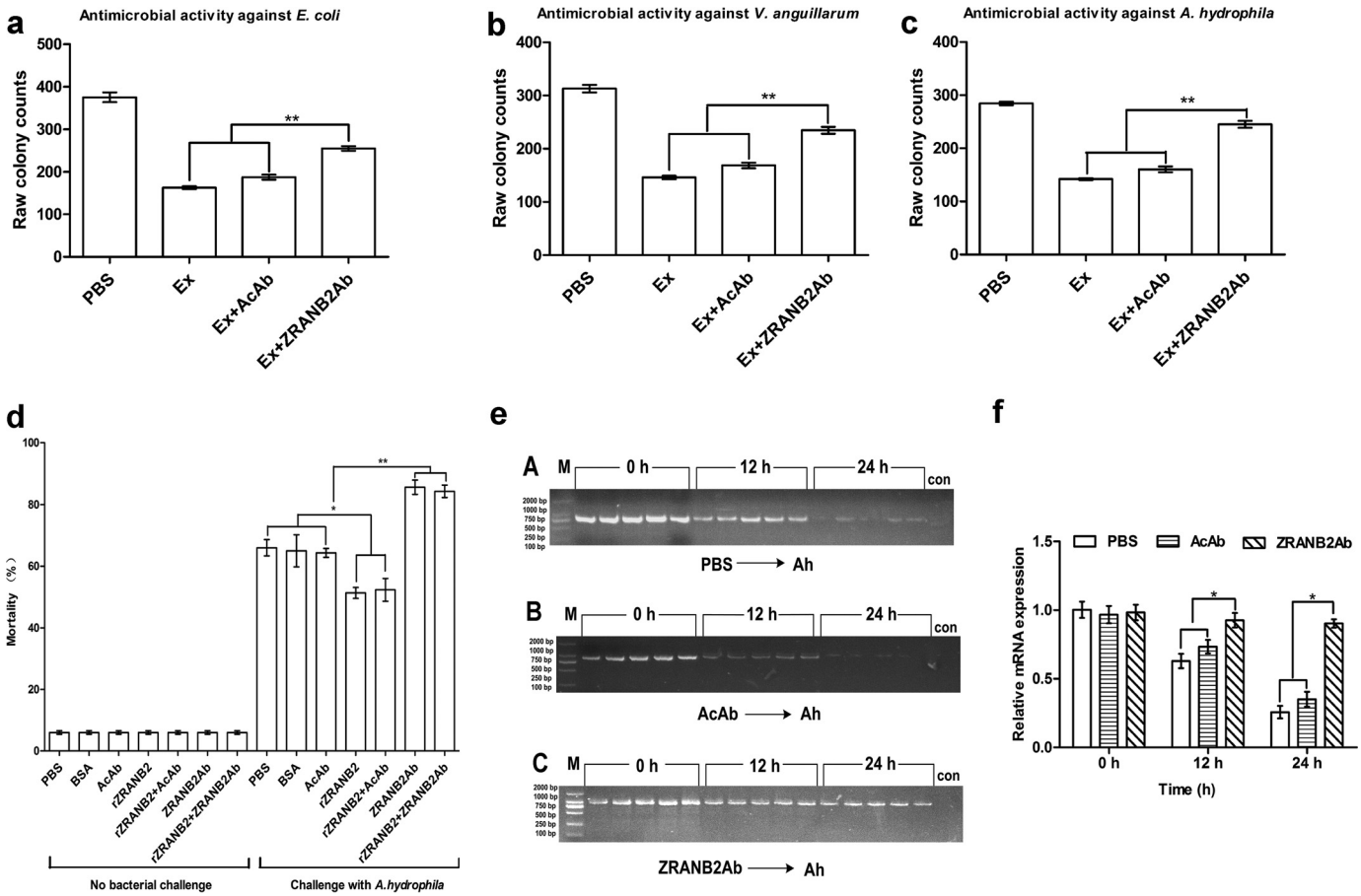

FIGURE 7. **Antibacterial activities of ZRANB2 against *E. coli*, *V. anguillarum*, and *A. hydrophila in vitro* and *in vivo*.** *a*, antimicrobial activity of the embryo extract against *E. coli*. *b*, antimicrobial activity of the embryo extract against *V. anguillarum*. *c*, antimicrobial activity of the embryo extract against *A. hydrophila*. *d*, the early (8-cell stage) embryos were first microinjected with PBS, BSA, anti-β-actin antibody (*AcAb*), anti-human ZRANB2 antibody (*ZRANB2Ab*), rZRANB2, and rZRANB2 plus AcAb or rZRANB2 plus ZRANB2Ab and then challenged by injection with live *A. hydrophila*. The development of the embryos was observed, and the cumulative mortality rate was calculated at 24 h after bacterial injection. *e*, PCR analysis of *A. hydrophila* 16s rRNA gene. The 8-cell stage embryos were microinjected with live *A. hydrophila*, and five embryos were collected each time at 0, 12, and 24 h after the bacterial injection. Total DNA was isolated from each embryo and used as the template to amplify the specific region of the *A. hydrophila* 16s rRNA gene. All of the PCR products were electrophoresed in 1% agarose, and the bands were recorded using the gel imaging system. *A*, embryos injected with *A. hydrophila* only; *B*, embryos injected with anti-β-actin antibody followed by injection with *A. hydrophila*; *C*, embryos injected with anti-human ZRANB2 antibody followed by injection with *A. hydrophila*. *M*, marker; *con*, control. *f*, expression patterns of *A. hydrophila* 16s rRNA gene. All data were expressed as mean values ± S.D. ($n = 3$). The data are from three independent experiments performed in triplicate. The *bars* represent the mean ± S.D. *, means significant difference ($p < 0.05$); **, extremely significant difference ($p < 0.01$). *Ex*, embryo extract; *AcAb*, anti-β-actin antibody; *ZRANB2Ab*, anti-human ZRANB2 antibody.

each embryo is sufficient enough to kill potential pathogens *in vivo*, at least at the initial 24 hpf. Notably, ZRANB2 was apparently not distributed homogenously in the embryos but was restricted in the blastoderm of early embryos and in the epidermis and neural tube of larvae. Therefore, the concentration of ZRANB2 in these sites of the embryos is certainly higher than 10 μg/ml, which may greatly strengthen the antibacterial activity therein.

The N-terminal 11–37 Residues Are Critical for Antibacterial Activity of ZRANB2—The deletion of the N-terminal 37 residues resulted in an almost complete loss of the antibacterial activity of ZRANB2 against *E. coli*, *V. anguillarum*, and *A. hydrophila* (Figs. 8, *a–d*, and 9*c*), suggesting that the N-terminal 37 residues are important for antibacterial activity. This may be due to the fact that the deletion of the N-terminal 37 residues resulted in the loss of the Zn^{2+}-binding site, and thus the remaining C-terminal 161 residues without a Zn^{2+}-binding site may not form correct three-dimensional structures. By contrast, synthesized $Z_{1/37}$ and $Z_{11/37}$ both retained a large antibacterial activity against *E. coli*, *V. anguillarum*, and *A. hydrophila* in the presence of Zn^{2+} (Figs. 8, *e–j*, and 9, *b* and *d*). Specifically, the IC_{50} values of $Z_{1/37}$ and $Z_{11/37}$ against *A. hydrophila* were ~9.3 and ~8.5 μg/ml, respectively, which are just slightly lower than that (~9.7 μg/ml) of full-length rZRANB2. It is interesting to note that $Z_{38/198}$ containing the second ZnF_RBZ domain had little antibacterial activity, whereas both $Z_{1/37}$ and $Z_{11/37}$ containing the first ZnF_RBZ domain retained the antibacterial activity. The reason for this difference is probably because the second ZnF_RBZ domain in ZRANB2 has no Zn^{2+}-binding site (Fig. 3*b*). It is also notable that $Z_{1/37}$ and $Z_{11/37}$ possess affinity to LPS (Fig. 8, *l* and *m*), consistent with the fact that they both retained the antimicrobial activity, whereas $Z_{38/198}$ lost the affinity to LPS (Fig. 8*k*), agreeing with the fact that it had little antimicrobial activity. These findings suggest that the antibacterial activity of $Z_{1/37}$ and $Z_{11/37}$, as well as rZRANB2, is related to their capacity to bind to LPS. Altogether, these data indicate that the N-terminal 37 residues, especially residues 11–37 comprising the first ZnF_RBZ

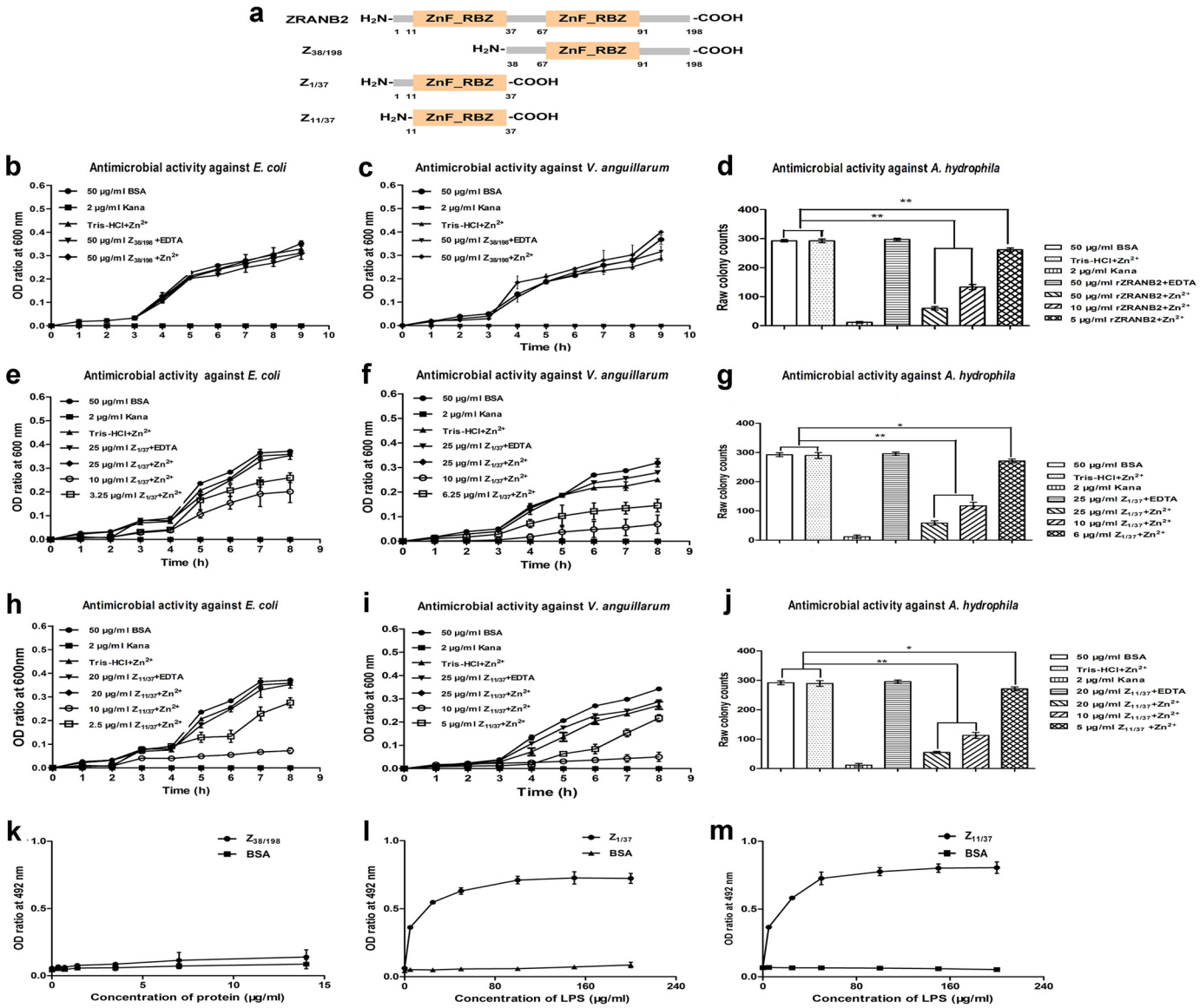

FIGURE 8. **Diagram showing zebrafish ZRANB2 truncation, analyses of bioactivity of $Z_{1/37}$, $Z_{11/37}$, and $Z_{38/198}$ against *E. coli*, *V. anguillarum*, and *A. hydrophila*, and binding of $Z_{38/198}$, $Z_{1/37}$, and $Z_{11/37}$ to LPS.** *a*, diagram showing zebrafish ZRANB2 truncation. *b–d*, antibacterial activity of $Z_{38/198}$ against *E. coli*, *V. anguillarum*, and *A. hydrophila*. *e–g*, antibacterial activity of $Z_{1/37}$ against *E. coli*, *V. anguillarum*, and *A. hydrophila*. *h–j*, antibacterial activity of $Z_{11/37}$ against *E. coli*, *V. anguillarum*, and *A. hydrophila*. *, significant difference ($p < 0.05$); **, extremely significant difference ($p < 0.01$). *k–m*, binding of $Z_{38/198}$, $Z_{1/37}$, and $Z_{11/37}$ to LPS. BSA was treated at the same concentrations as the control. All data were expressed as mean values ± S.D. ($n = 3$). The data are from three independent experiments performed in triplicate. The *bars* represent the mean ± S.D.

domain itself, are the core region indispensable for both antimicrobial activity and binding to LPS.

When the embryos were each microinjected with $Z_{1/37}$, $Z_{11/37}$, or $Z_{38/198}$, approximately ~94% of the embryos developed normally. By contrast, the challenge with live *A. hydrophila* caused a significant increase in the mortality rate of the embryos injected with $Z_{38/198}$, PBS, or BSA, with a 24-h cumulative mortality rate of ~66, 68.3, and 63.7%, respectively; but the same challenge induced only ~51.3 and 47.7% cumulative mortality at 24 h in the embryos injected with $Z_{1/37}$ or $Z_{11/37}$ (Fig. 10). Moreover, the embryo-protecting role of $Z_{1/37}$ and $Z_{11/37}$ was counteracted by the co-injection of anti-ZRANB2 antibody but not by co-injection of anti-actin antibody (Fig. 10). It is thus clear that $Z_{1/37}$ and $Z_{11/37}$, with antimicrobial activity *in vitro*, are also involved in the antimicrobial activity of developing embryos, whereas $Z_{38/198}$, with no antibacterial activity *in vitro*, exhibits no antibacterial activity *in vivo*.

Discussion

Information regarding the functions and mechanisms of ZRANB2 proteins remains rather limited to date. Here we clearly demonstrate that zebrafish ZRANB2 is a novel LPS-binding protein stored abundantly in the eggs/embryos. It can function as a pattern recognition receptor (PRR), which recognizes potential Gram-negative pathogens through interaction with LPS via lipid A. The nature of ZRANB2 may have an important physiological significance. Great advances have been made recently in identifying pattern recognition molecules, but few of them have been tested for their existence in early embryos (55). Our data show that ZRANB2 is a new PRR functioning in the eggs and early embryos

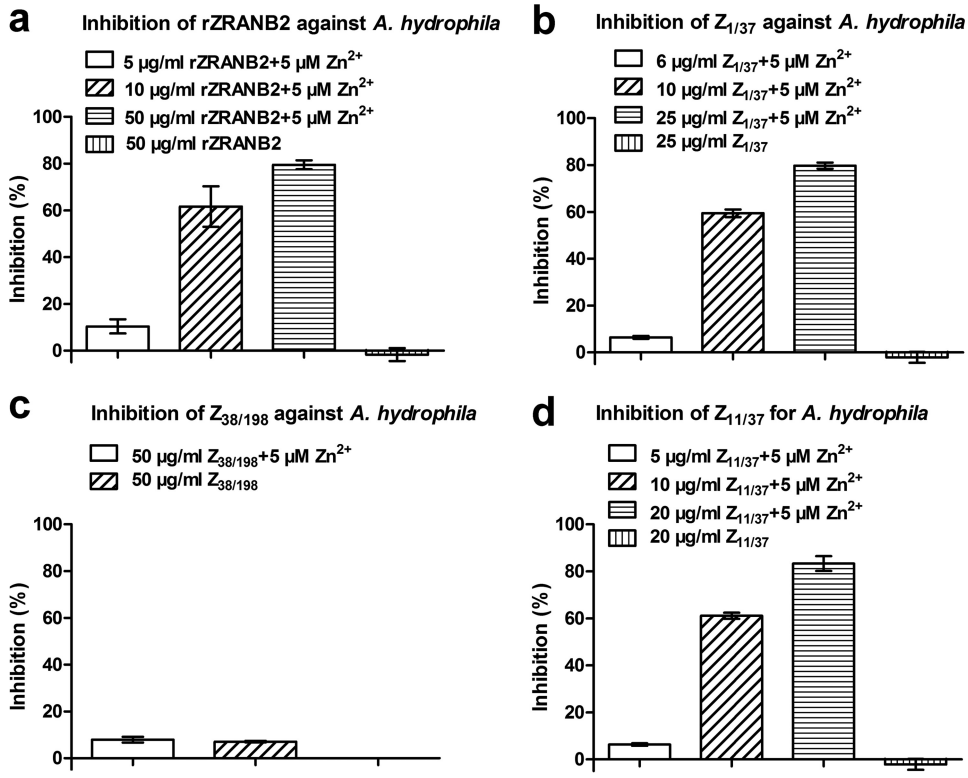

FIGURE 9. **Antimicrobial activity of rZRANB2 and its truncated peptides against *A. hydrophila*.** *a,* inhibition of rZRANB2 against *A. hydrophila*. *b,* inhibition of $Z_{1/37}$ against *A. hydrophila*. *c,* inhibition of $Z_{38/198}$ against *A. hydrophila*. *d,* inhibition of $Z_{11/37}$ against *A. hydrophila*. Each point in the graph represents the mean ± S.D. ($n = 3$). The data are from three independent experiments performed in triplicate. The *bars* represent the mean ± S.D.

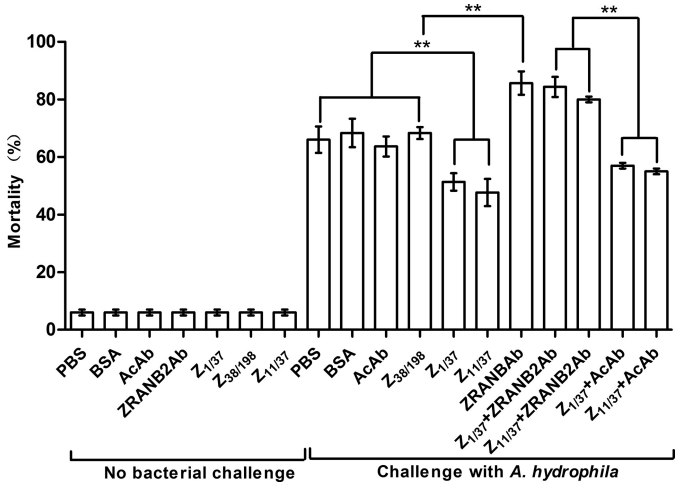

FIGURE 10. **The *in vivo* bioactivity of $Z_{1/37}$, $Z_{11/37}$, and $Z_{38/198}$.** The early (8-cell stage) embryos were first microinjected with PBS, BSA, anti-β-actin antibody (*AcAb*), anti-human ZRANB2 antibody (*ZRANB2Ab*), $Z_{1/37}$, $Z_{11/37}$, and $Z_{38/198}$ and then challenged by injection with live *A. hydrophila*. The development of the embryos was observed, and the cumulative mortality rate was calculated at 24 h after injection. **, extremely significant difference ($p < 0.01$). All data were expressed as mean values ± S.D. ($n = 3$). The data are from three independent experiments performed in triplicate. The *bars* represent the mean ± S.D.

of zebrafish. However, it must be pointed out that ZRANB2 may function only when pathogens have penetrated the embryos/larvae, as it is localized in the cytoplasm.

An important part of innate immunity is that quite a few proteins show antibacterial activity in addition to having an immune recognition function. These proteins play essential roles in host nonspecific defenses by preventing or limiting infections via their capacity to recognize potential pathogens; most of these proteins also exert antibacterial effects by interacting with and destabilizing either the bacterial cell wall or the plasma membranes, leading to cell death eventually. Another important finding of our study is that ZRANB2 is not only a PRR capable of binding to Gram-negative bacteria but also an effector molecule capable of lyzing pathogenic *A. hydrophila*. Because an injection of exogenous rZRANB2 into early embryos promotes their resistance to pathogenic *A. hydrophila* challenge, and this bacteria-resistant activity is clearly reduced by the co-injection of anti-ZRANB2 antibody, we thus propose that ZRANB2 may defend early embryos *in vivo* against pathogenic attacks by the same mechanisms via binding to and lyzing invading pathogens.

Fishes represent basal vertebrates that have an innate and adaptive system comparable with that of mammals. Currently, little information is available regarding the role of ZRANB2 in mammalian embryonic development, although it has been shown to be a developmentally regulated factor expressed in juxtaglomerular cells (37). Given the high conservation rate of ZRANB2 from fish to mammals, we thus speculate that mammalian ZRANB2 may also play a similar role in early development. However, this deserves further study in the future.

Proteins are built as chains of amino acids, which then fold into unique three-dimensional shapes; and the final folded forms of proteins are well adapted for their functions. It is notable that the N-terminal 37 residues, especially those 26 residues comprising the first ZnF_RBZ domain *per se*, are the core struc-

ture contributing to the antimicrobial activity of ZRANB2. The first ZnF_RBZ domain of zebrafish ZRANB2 has a Zn^{2+}-binding site, whereas the second domain does not, as revealed by our three-dimensional structure prediction (Fig. 3*b*). This may be the reason that the N-terminal 37 residues containing the first ZnF_RBZ possess antibacterial activity, but the C-terminal 161 residues containing the second ZnF_RBZ do not. It is also notable that the antibacterial activity against *E. coli*, *V. anguilarum*, and *A. hydrophila* and the affinity to LPS co-exist in both $Z_{1/37}$ and $Z_{11/37}$ as well as rZRANB2, but neither the antibacterial activity nor the affinity to LPS are present in $Z_{38/198}$, suggesting the presence of a correlation between antibacterial activity and LPS binding activity. Possibly, this correlation indicates that the functional sites of rZRANB2, $Z_{1/37}$, and $Z_{11/37}$ may be involved simultaneously in multiple activities, including binding to microbial signature molecule LPS and destabilizing/disrupting bacterial cell membranes.

In conclusion, this study is the first to demonstrate that ZRANB2 is a novel maternal LPS-binding protein associated with the antibacterial defense of early embryos in zebrafish; and then it elucidates that ZRANB2 is a PRR capable of identifying LPS and an antibacterial effector molecule capable of inhibiting the growth of Gram-negative bacteria. Moreover, our study reveals that the N-terminal 26 residues with the ZnF_RBZ domain are critical for ZRANB2 antibacterial activity. This work also provides a new angle for the study of the immunological roles of zinc finger proteins, which are widely distributed in various animals.

Author Contributions—S. Z. and X. W. designed the experiments and wrote the paper. X. W. and X. D. performed the experiments. X. W., X. D., H. L., and S. Z. analyzed the data. All authors approved the final version of the manuscript.

Acknowledgments—We are grateful to Mingzhuang Zhu for technical aid in flow cytometry and to Yunsi Kang, Haibo Xie, and Dong Feng for help with immunohistochemistry.

References

1. Brock, F. V., Crawford, K. C., Elliott, R. L., Cuperus, G. W., Stadler, S. J., Johnson, H. L., Eilts, M. D. (1995) The Oklahoma Mesonet: a technical overview. *J. Atmos. Oceanic Technol.* **12,** 5
2. Plumb, J. A. (1994) *Health Maintenance of Cultured Fishes: Principal Microbial Diseases*, CRC Press, Boca Raton, FL
3. Plumb, J. A. (1978) Epizootiology of channel catfish virus disease. *Mar. Fish. Rev.* **40,** 26–29
4. Haig, S. J., Davies, R. L., Welch, T. J., Reese, R. A., and Verner-Jeffreys, D. W. (2011) Comparative susceptibility of Atlantic salmon and rainbow trout to *Yersinia ruckeri*: relationship to oantigen serotype and resistance to serum killing. *Vet. Microbiol.* **147,** 155–161
5. Ellis, A. E., Stapleton, K. J., and Hastings, T. S. (1988) The humoral immune response of rainbow trout (*Salmo gairdneri*) immunised by various regimes and preparations of *Aeromonas salmonicida* antigens. *Vet. Immunol. Immunopathol.* **19,** 153–164
6. Magnadóttir, B., Lange, S., Steinarsson, A., and Gudmundsdóttir, S. (2004) The ontogenic development of innate immune parameters of cod (*Gadus morhua* L.). *Comp. Biochem. Physiol. B Biochem. Mol. Biol.* **139,** 217–224
7. Zhang, P., Zucchelli, M., Bruce, S., Hambiliki, F., Stavreus-Evers, A., Levkov, L., Skottman, H., Kerkelä, E., Kere, J., and Hovatta, O. (2009) Transcriptome profiling of human pre-implantation development. *PLoS One* **4,** e7844
8. Zhang, S., Wang, Z., and Wang, H. (2013) Maternal immunity in fish. *Dev. Comp. Immunol.* **39,** 72–78
9. Bly, J. E., Grimm, A. S., and Morris, I. G. (1986) Transfer of passive immunity from mother to young in a teleost fish: haemagglutinating activity in the serum and eggs of plaice, *Pleuronectes platessa* L. *Comp. Biochem. Physiol. A Comp. Physiol.* **84,** 309–313
10. Breuil, G., Vassiloglou, B., Pepin, J. F., and Romestand, B. (1997) Ontogeny of IgM-bearing cells and changes in the immunoglobulin M-like protein level (IgM) during larval stages in sea bass (*Dicentrarchus labrax*). *Fish Shellfish Immunol.* **7,** 29–43
11. Castillo, A., Sánchez, C., Dominguez, J., Kaattari, S. L., and Villena, A. J. (1993) Ontogeny of IgM and IgM-bearing cells in rainbow trout. *Dev. Comp. Immunol.* **17,** 419–424
12. Fuda, H., Hara, A., Yamazaki, F., and Kobayashi, K. (1992) A peculiar immunoglobulin M (IgM) identified in eggs of chum salmon (*Oncorhynchus keta*). *Dev. Comp. Immunol.* **16,** 415–423
13. Hanif, A., Yasmeen, A., and Rajoka, M. I. (2004) Induction, production, repression, and de-repression of exoglucanase synthesis in *Aspergillus niger*. *Bioresour. Technol.* **94,** 311–319
14. Mor, A., and Avtalion, R. R. (1990) Transfer of antibody activity from immunized mother to embryo in tilapias. *J. Fish Biol.* **37,** 249–255
15. Olsen, Y. A., and Press, C. Mcl. (1997) Degradation kinetics of immunoglobulin in the egg, alevin, and fry of Atlantic salmon, *Salmo salar* L., and the localisation of immunoglobulin in the egg. *Fish Shellfish Immunol.* **7,** 81–91
16. Picchietti, S., Taddei, A. R., Scapigliati, G., Buonocore, F., Fausto, A. M., Romano, N., Mazzini, M., Mastrolia, L., and Abelli, L. (2004) Immunoglobulin protein and gene transcripts in ovarian follicles throughout oogenesis in the teleost *Dicentrarchus labrax*. *Cell Tissue Res.* **315,** 259–270
17. Picchietti, S., Abelli, L., Buonocore, F., Randelli, E., Fausto, A. M., Scapigliati, G., and Mazzini, M. (2006) Immunoglobulin protein and gene transcripts in sea bream (*Sparus aurata* L.) oocytes. *Fish Shellfish Immunol.* **20,** 398–404
18. Swain, S. L., Agrewala, J. N., Brown, D. M., Jelley-Gibbs, D. M., Golech, S., Huston, G., Jones, S. C., Kamperschroer, C., Lee, W. H., McKinstry, K. K., Román, E., Strutt, T., and Weng, N. P. (2006) CD4+ T-cell memory: generation and multi-faceted roles for CD4+ T cells in protective immunity to influenza. *Immunol. Rev.* **211,** 8–22
19. van Loon, A. M., Heessen, F. W., van der Logt, J. T., and van der Veen, J. (1981) Direct enzyme-linked immunosorbent assay that uses peroxidase-labeled antigen for determination of immunoglobulin M antibody to cytomegalovirus. *J. Clin. Microbiol.* **13,** 416–422
20. Wang, F. Y., Bromm, V., Greif, T. H., Stacy, A., Dai, Z. G., Loeb, A., and Cheng, K. S. (2012) Probing pre-galactic metal enrichment with high-redshift γ-ray bursts. *Astrophys. J. Suppl. Ser.* **760,** 27
21. Bildfella, R. J., Markhama, F. R., and Johnsona, G. R. (1992) Purification and partial characterization of a rainbow trout egg lectin. *J. Aquat. Anim. Health* **4,** 97–105
22. Dong, C. H., Yang, S. T., Yang, Z. A., Zhang, L., and Gui, J. F. (2004) A C-type lectin associated and translocated with cortical granules during oocyte maturation and egg fertilization in fish. *Dev. Biol.* **265,** 341–354
23. Hasan, I., Kabir, S. R., Haque, M. A., and Absar, N. (2009) Biochemical analysis and physico chemical stability of a partially purified lectin from *Hilsha* eggs. *J. Bio-sci.* **17,** 35–40
24. Jung, Y. J., Isaacs, J. S., Lee, S., Trepel, J., and Neckers, L. (2003) IL-1β-mediated up-regulation of HIF-1α via an NFκB/COX-2 pathway identifies HIF-1 as a critical link between inflammation and oncogenesis. *FASEB J.* **17,** 2115–2117
25. Tateno, H., Yamaguchi, T., Ogawa, T., Muramoto, K., Watanabe, T., Kamiya, H., and Saneyoshi, M. (2002) Immunohistochemical localization of rhamnose-binding lectins in the steelhead trout (*Oncorhynchus mykiss*). *Dev. Comp. Immunol.* **26,** 543–550
26. Wang, Z., and Zhang, S. (2010) The role of lysozyme and complement in the antibacterial activity of zebrafish (*Danio rerio*) egg cytosol. *Fish Shellfish Immunol.* **29,** 773–777
27. Yousif, A. N., Albright, L. J., and Evelyn, T. P. T. (1991) Occurrence of lysozyme in the eggs of Coho salmon *Oncorhynchus kisutch*. *Dis. Aquat. Org.* **10,** 45–49

28. Yousif, A. N., Albright, L. J., and Evelyn, T. P. T. (1994) *In vitro* evidence for the antibacterial role of lysozyme in salmonid eggs. *Dis. Aquat. Org.* **19,** 15–19
29. Wang, S., Wang, Y., Ma, J., Ding, Y., and Zhang, S. (2011) Phosvitin plays a critical role in the immunity of zebrafish embryos via acting as a pattern recognition receptor and an antimicrobial effector. *J. Biol. Chem.* **286,** 22653–22664
30. Zhang, J., and Zhang, S. (2011) Lipovitellin is a non-self recognition receptor with opsonic activity. *Mar. Biotechnol.* **13,** 441–450
31. Ellingsen, S., Laplante, M. A., König, M., Kikuta, H., Furmanek, T., Hoivik, E. A., and Becker, T. S. (2005) Large-scale enhancer detection in the zebrafish genome. *Development* **132,** 3799–3811
32. Bernard, H. U., Burk, R. D., Chen, Z., van Doorslaer, K., zur Hausen, H., and de Villiers, E. M. (2010) Classification of papillomaviruses (PVs) based on 189 PV types and proposal of taxonomic amendments. *Virology* **401,** 70–79
33. Huttenhuis, H. B., Ribeiro, A. S., Bowden, T. J., Van Bavel, C., Taverne-Thiele, A. J., and Rombout, J. H. (2006) The effect of oral immuno-stimulation in juvenile carp (*Cyprinus carpio* L.). *Fish Shellfish Immunol.* **21,** 261–271
34. Sun, C., Hu, L., Liu, S., Hu, G., and Zhang, S. (2013) Antiviral activity of phosvitin from zebrafish *Danio rerio*. *Dev. Comp. Immunol.* **40,** 28–34
35. Wang, Z., Zhang, S., and Wang, G. (2008) Response of complement expression to challenge with lipopolysaccharide in embryos/larvae of zebrafish *Danio rerio*: acquisition of immunocompetent complement. *Fish Shellfish Immunol.* **25,** 264–270
36. Wang, Z., Zhang, S., Tong, Z., Li, L., and Wang, G. (2009) Maternal transfer and protective role of the alternative complement components in Zebrafish *Danio rerio*. *PLoS One* **4,** e4498
37. Karginova, E. A., Pentz, E. S., Kazakova, I. G., Norwood, V. F., Carey, R. M., and Gomez, R. A. (1997) *Zis*: a developmentally regulated gene expressed in juxtaglomerular cells. *Am. J. Physiol. Renal Physiol.* **273,** F731–F738
38. Adams, D. J., van der Weyden, L., Mayeda, A., Stamm, S., Morris, B. J., and Rasko, J. E. (2001) ZNF265: a novel spliceosomal protein able to induce alternative splicing. *J. Cell Biol.* **154,** 25–32
39. Mangs, A. H., and Morris, B. J. (2007) The human pseudoautosomal region (PAR): origin, function, and future. *Curr. Genomics* **8,** 129–136
40. Ohte, S., Kokabu, S., Iemura, S., Sasanuma, H., Yoneyama, K., Shin, M., Suzuki, S., Fukuda, T., Nakamura, Y., Jimi, E., Natsume, T., and Katagiri, T. (2012) Identification and functional analysis of Zranb2 as a novel Smad-binding protein that suppresses BMP signaling. *J. Cell Biol.* **113,** 808–814
41. Yang, Y. H., Markus, M. A., Mangs, A. H., Raitskin, O., Sperling, R., and Morris, B. J. (2013) ZRANB2 localizes to supraspliceosomes and influences the alternative splicing of multiple genes in the transcriptome. *Mol. Biol. Rep.* **40,** 5381–5395
42. Chiou, S. T., Chen, Y. W., Chen, S. C., Chao, C. F., and Liu, T. Y. (2000) Isolation and characterization of proteins that bind to galactose, lipopolysaccharide of *Escherichia coli*, and protein A of *Staphylococcus aureus* from the hemolymph of *tachypleus tridentatus*. *J. Biol. Chem.* **275,** 1630–1634
43. Minoda, Y., Saeki, K., and Aki, D. (2006) A novel Zinc finger protein, ZCCHC11, interacts with TIFA and modulates TLR signaling. *Mol. Cell Biol. Res. Commun.* **344,** 1023–1030
44. Choi, S., Baik, J. E., Jeon, J. H., Cho, K., Seo, D. G., Kum, K. Y., Yun, C. H., and Han, S. H. (2011) Identification of *Porphyromonas gingivalis* lipopolysaccharide-binding proteins in human saliva. *Mol. Immunol.* **48,** 2207–2213
45. Chenna, R., Sugawara, H., Koike, T., Lopez, R., Gibson, T. J., Higgins, D. G., and Thompson, J. D. (2003) Multiple sequence alignment with the Clustal series of programs. *Nucleic Acids Res.* **31,** 3497–3500
46. Livak, K. J., and Schmittgen, T. D. (2001) Analysis of relative gene expression data using real-time quantitative PCR and the $2^{-\Delta\Delta Ct}$ method. *Methods* **25,** 402–408
47. Thisse, C., and Thisse, B. (2008) High-resolution in situ hybridization to whole-mount zebrafish embryos. *Nat. Protoc.* **3,** 59–69
48. Zhang, Y., Li, W., Ou, L., Wang, W., Delyagina, E., Lux, C., Sorg, H., Riehemann, K., Steinhoff, G., and Ma, N. (2012) Targeted delivery of human VEGF gene via complexes of magnetic nanoparticle-adenoviral vectors enhanced cardiac regeneration. *PLoS One* **7,** e39490
49. Gao, Z., Li, M., Ma, J., and Zhang, S. (2014) An amphioxus gC1q protein binds human IgG and initiates the classical pathway: implications for a C1q-mediated complement system in the basal chordate. *Eur. J. Immunol.* **44,** 3680–3695
50. Li, Z., Zhang, S., and Liu, Q. (2008) Vitellogenin functions as a multivalent pattern recognition receptor with an opsonic activity. *PLoS One* **3,** e1940
51. Yao, F., Li, Z., Zhang, Y., and Zhang, S. (2012) A novel short peptidoglycan recognition protein in amphioxus: Identification, expression and bioactivity. *Dev. Comp. Immunol.* **38,** 332–341
52. Liang, Y., Zhang, S., and Wang, Z. (2009) Alternative complement activity in the egg cytosol of amphioxus *Branchiostoma belcheri*: evidence for the defense role of maternal complement components. *PLoS One* **4,** e4234
53. Laity, J. H., Lee, B. M., and Wright, P. E. (2001) Zinc finger proteins: new insights into structural and functional diversity. *Curr. Opin. Struct. Biol.* **11,** 39–46
54. Ostermeier, C., and Brunger, A. T. (1999) Structural basis of Rab effector specificity: crystal structure of the small G protein Rab3A complexed with the effector domain of rabphilin-3A. *Cell* **96,** 363–374
55. Akira, S., Uematsu, S., and Takeuchi, O. (2006) Pathogen recognition and innate immunity. *Cell* **124,** 783–801